Extension of Ammonium and Nitrate Wet-Fall Deposition Models for the Chesapeake Bay Watershed

FINAL REPORT

Prepared By:

Jeffrey W. Grimm, The Pennsylvania State University

This report was funded by and prepared for the
United States Environmental Protection Agency, Chesapeake Bay Program and the Pennsylvania Department of Environmental Protection

6 January 2017

Acknowledgments

Funding for this project was provided by the United States Environmental Protection Agency's Chesapeake Bay Program Office and the Pennsylvania Department of Environmental Protection under Contract 4400008014. We extend our thanks to Lewis Linker and the staff of the Chesapeake Bay Program Office for their assistance in acquiring data sets essential to this project, for their insights into how the results of our analyses are used, and for their suggestions on how make those results useful for management decision making.

Introduction

Grimm and Lynch (2005) demonstrated that estimates of daily ammonium and nitrate wet-fall concentration to the river modeling zones of the Chesapeake Bay Watershed region could be improved, relative to earlier efforts, by incorporating land use/land cover composition, quantitative topographic characteristics, and detailed precipitation histories as predictors in regression models relating ionic concentrations to sparsely-sampled, weekly precipitation chemistry observations from the National Atmospheric Deposition Program/National Trends Network (NADP/NTN). However, considerable variation between the estimates of wet-fall concentration and wet deposition obtained from those models and observed values remained, particularly for the ammonium estimates. Furthermore, some of the statistical relationships between broadly defined categories of land use/land cover composition provided by the U.S. Geological Survey's National Land Cover Database (NLCD) and patterns of wet deposition of ammonium and nitrate were ambiguous.

One limitation of our initial modeling effort was that the NADP/NTN sample data used was restricted to sites whose locations were selected to represent emissions and deposition levels on a broad, regional scale and; as such, did not generally reflect local ammonium emissions from agricultural sources. On a local scale, emissions from agricultural activities, particularly livestock production and fertilizer application to croplands, can dramatically influence the atmospheric ammonia levels available for deposition. Many of the discrepancies between observed daily ammonium depositions and estimates from the previous models likely reflect the intensity and timing of adjacent agricultural activities. Deposition monitoring sites that are more likely to reflect the influence of local emissions from livestock and crop production have been established within the Chesapeake Bay Watershed region since the original development of our daily ammonium and nitrate wet-fall deposition models. One such site, PA47, was established on a dairy farm in Lancaster County, PA, near Millersville University. Ammonium wet-fall concentrations and wet deposition at this site in 2004 was nearly double that of any other site located in the Chesapeake Bay Watershed. The annual ammonium concentration in precipitation at PA47 was the highest of all NADP/NTN sites located east of the Ohio River; including one of the North Carolina sites that is severely impacted by swine production. Incorporation of precipitation chemistry observations from the expanded network of monitoring stations along with a more detailed accounting of agricultural activities in daily ammonium wet-fall concentration and deposition models is expected to improve their predictive ability.

Our preceding model development focused on estimating daily wet-fall concentrations of ammonium and nitrate using measures of long-term (multi-year) and seasonal trends in precipitation chemistry, geographic location, surrounding land use and usage intensities, precipitation volume, and antecedent precipitation event histories. The abilities of these factors to predict wet deposition arise primarily from their relationship to either 1) the spatial and temporal distribution of emissions of ammonium and nitrate precursors from sources located within the CBW or in areas upwind from the watershed and 2) the chronology and characteristics of precipitation events. However, other meteorological phenomena that were not incorporated into the wet-fall concentration models can have significant influences on the flux of ammonium and nitrate delivered to the CBW by individual precipitation events. The volume, duration, and frequency of precipitation events have an obvious role in determining wet-fall concentration and wet deposition rates by scavenging the atmospheric load of ammonium and nitrate precursors and carrying the material to the surface. Although measurements of precipitation volume are represented in the previous daily wet deposition models (Grimm and Lynch, 2005), they do not describe all of the characteristics of a precipitation event and its history that determine the flux of nitrogen it will deposit. For example, Walker et al (1999) found that weekly wet-fall concentrations of ammonium at two NADP/NTN sites in North Carolina were approximately 44 percent higher when the trajectories of at least 25 percent of the weekly precipitation events traversed a multi-

county region where swine production was most intensive. We anticipate that daily wet-fall concentration levels of ammonium in the CBW will be even more sensitive to interactions between storm trajectories and emission sources than was demonstrated by the relationship between weekly mean concentration and the simple categorical storm tracking employed in the North Carolina study. A high-resolution mapping of livestock production and cropland areas combined with high frequency rainfall estimates and multi-level estimates of wind velocities from numerical weather models, presents the opportunity to construct a detailed history of the pathways followed by each precipitation event's component air masses as they pass over and potentially absorb emissions released from the delineated source areas.

The influence of temperature on the atmospheric flux of nitrogen to the CBW has not yet been addressed by the initial daily wet-fall concentration models. We believe that incorporation of temperature parameters may be particularly beneficial to the ammonium model. Addiscott (1983) and others have demonstrated that rising soil temperature increases the rate of ammonification of nutrients within the soil and, thereby, accelerates the release of ammonia into the atmosphere. Furthermore, the release of ammonia from waste lagoons, such as those associated with livestock production areas, has also been shown to increase with rising water temperature (Harper and Sharpe, 1997). Additionally, the rate of conversion and volatilization of nitrogen-containing fertilizer compounds applied to croplands is expected to be temperature-dependent. Therefore, we expect that the inclusion of temperature data in our daily ammonium deposition model will significantly improve its performance by predicting changes in the availability of atmospheric ammonia for absorption and deposition by precipitation.

In this report we document the refinement and extension of the our previous daily ammonium and nitrate wet-fall concentration regression models for the CBW region (Grimm and Lynch, 2005; Grimm and Lynch, 2007). The revised models are referred, hereafter, as Phase 6 models and include:

1) an expanded set of precipitation chemistry observations that not only spans a longer time period (1984 through 2014 vs. 1984 through 2005), but also includes data from a greater number of monitoring locations that represent a wider range of local environments.

2) improved representation of the spatial distribution of land cover types, land use activities, and emission source locations that may influence local wet-fall concentrations by inclusion of land cover data from the 2001, 2006, and 2011 updates of the United States Geological Services National Land Cover Database (NLCD). These releases of the NLCD markedly improve discrimination between pasturelands and cultivated croplands relative to the 1992 NLCD used in our previous modeling effort (Grimm and Lynch, 2007).

3) nitrous oxide and ammonia emissions from the 1990, 1996, 1997, 1998, 1999, 2000, 2001, 2002, 2005, 2008, and 2011 editions of the United States Environmental Protection Angency's National Emissions Inventory (NEI) summaries (http://www.epa.gov/air/data/neidb.html). The 2002, 2005, 2008, and 2011 NEI releases were not available at the time of our previous analyses.

4) synthesis of a range of meteorological parameters to predict the timing and degree of influence of ammonia and nitrous oxide emissions released from a variety of area and point sources on local wet-fall concentrations of ammonium and nitrate.

5) hourly precipitation estimates from the NLDAS-2 model Xia et al (2012) to both define precipitation event volumes and to delineate the time, duration, and geospatial track of individual precipitation events. Estimates from the NLDAS-2 model represent a standardized source of precipitation volumes that is used throughout associated modeling efforts of nutrient flux through the Chesapeake Bay Program modeling domain.

Methods

Precipitation Chemistry Sample Data

The National Atmospheric Deposition Program (NADP) and the National Trends Network (NTN) have been in operation since 1978 and provide chemical analyses for weekly precipitation samples collected at over 220 monitoring sites across the United States in compliance with standardized sample collection and analytical protocols [NADP, 2002; Bigelow and Dossett, 1988; Peden et al, 1979]. Additional precipitation monitoring sites were operated according to NADP/NTN sampling protocol throughout Pennsylvania as the Pennsylvania Atmospheric Deposition Monitoring Network (PADM) from 1982 through 2010. Eighty-five of the NADP/NTN and PADM sites are located in or adjacent to the CBW modeling region, have been in active operation during all or part of the 1984 through 2014 study period, and satisfied the sampling completeness criterion of having valid chemical analyses for at least 75 percent of annual precipitation volume during one or more years in the study period (Fig. 1). Quality-controlled weekly measurements of wet-fall ammonium (NH_4^+) and nitrate (NO_3^-) concentrations and the corresponding precipitation volumes at these NADP/NTN and PADM sites constituted the precipitation chemistry data set used for model development. Because this modeling effort involves the development of daily concentration models of inorganic nitrogen compounds, only those weekly precipitation chemistry samples that were comprised of a single precipitation event were used for model development. In order to protect against inclusion of contaminated precipitation samples or erroneous lab analyses of concentration values, only those precipitation samples having cation:anion balances of 0.85 to 1.20 were included in model development. The following measures of precipitation event history were calculated for each precipitation chemistry sample from the daily precipitation records for each NADP/NTN station:

1) the number of days since the preceding precipitation event;
2) the volume of precipitation occurring in the preceding 12, 24, 48, 72, 96, 120, and 168-hour periods; and
3) the number of days having precipitation during the preceding 7-day period.

Seasonal Variation in Wet-fall Nitrogen Concentration

Seasonality is represented in the model by dividing each calendar year into six distinct bi-monthly periods. The first bi-monthly period corresponds to January and February and the sixth to November and December. The six seasonal time periods are represented in the linear regression model by an array of five binary indicator variables.

Land Use and Land Cover Data

In an effort to enhance the accuracy of modeled estimates of daily ammonium and nitrate concentrations, data describing local land use and spatial distributions of ammonia (NH_3) and nitrous oxide (NO_x) emissions were incorporated into the model development process. The 2001, 2006, and 2011 National Land Cover Data (NLCD) grids provide a 30-meter resolution land cover classification derived from satellite imagery that encompasses the CBW modeling region (Fig. 2;Vogelmann et a1, 1998). The NLCD data sets were used to calculate proportional representation of several land use categories within the proximities of 1, 2, 5, 10, 16, 32, and 64 km of each NADP/NTN site for evaluation as potential predictors of daily ammonium and nitrate wet-fall concentrations. The land use categories were quantified from the NLCD data were cultivated croplands; potential livestock production areas; light- and high-intensity residential development, industrial, and transportation corridors. Livestock production areas are

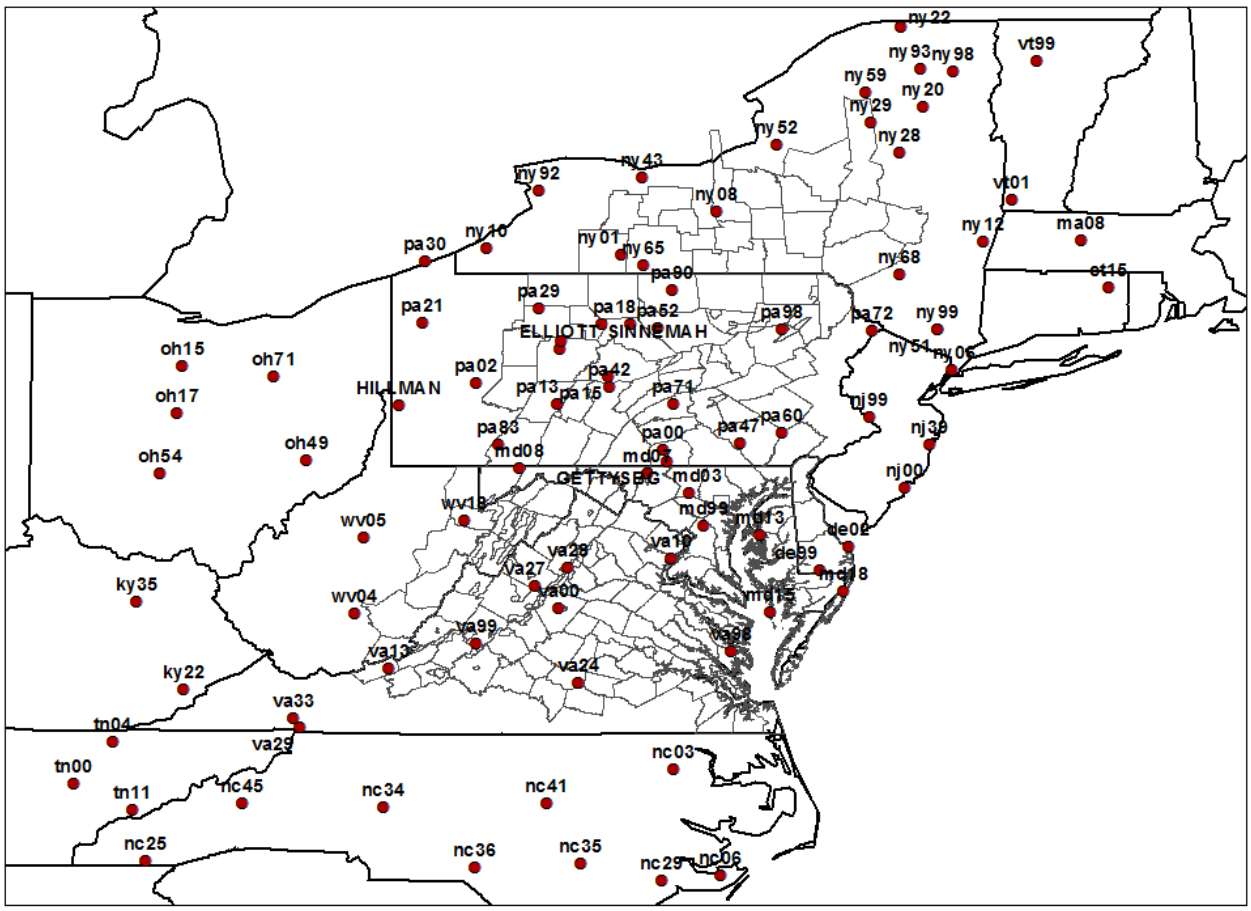

Figure 1. Locations of the 85 NADP/NTN and PADM precipitation chemistry monitoring sites used to provide data for the development and verification of the daily ammonium (NH_4^+) and nitrate (NO_3^-) wet-fall concentration models.

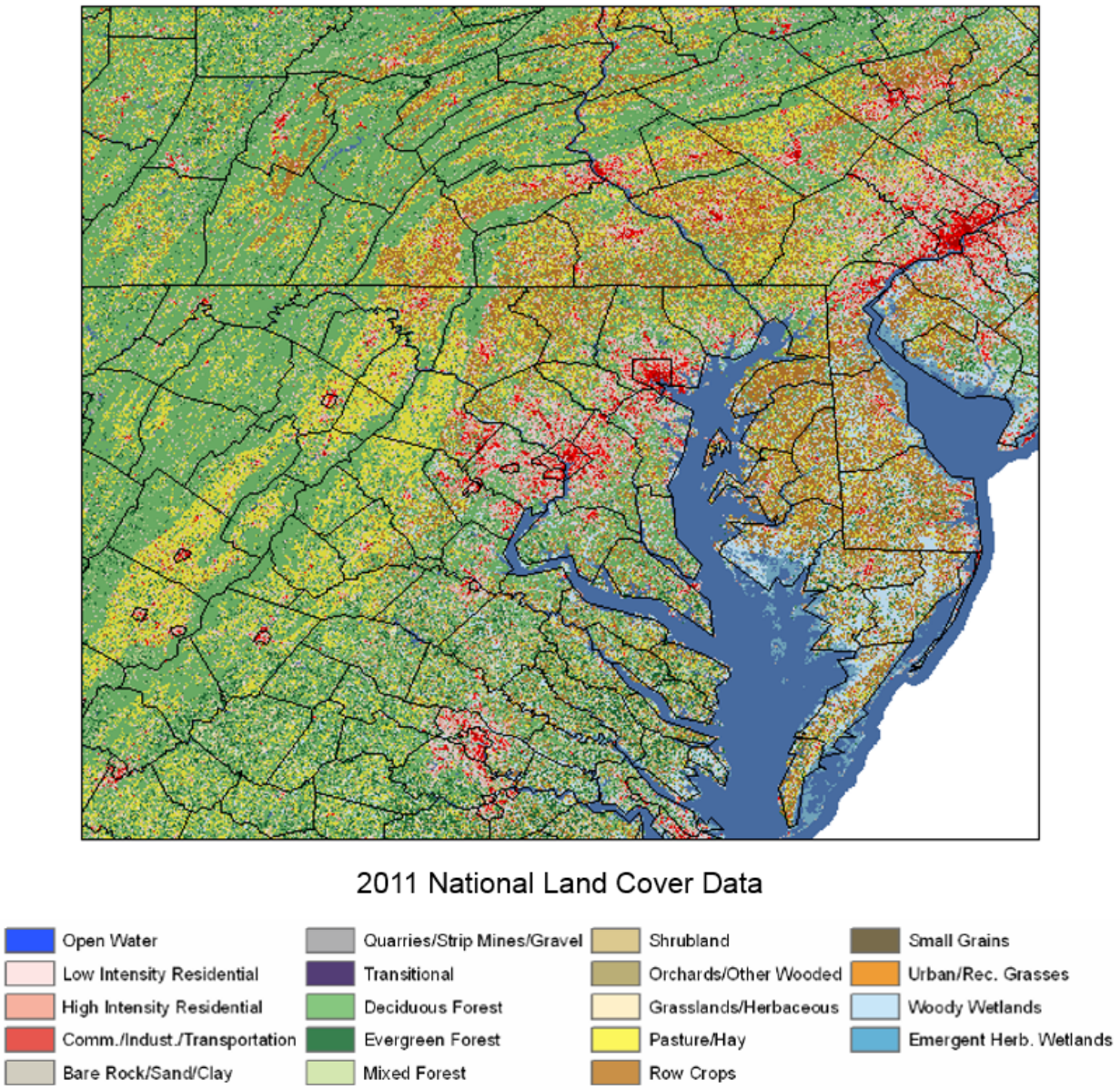

Figure 2. Subsection of 2011 National Land Cover Data set covering the central portion of the Chesapeake Bay Watershed modeling region.

not directly classified in the NLCD data. For this study, potential livestock production areas were identified for each NLCD grid cell based on surrounding NLCD land use classifications according to the following criteria:

1) At least 5 contiguous 30m NLCD grid cells classified as pasture or non-residential grassland
2) At least 50 percent of NLCD grids cells within 600 meters classified as pasture, cropland, or non-residential grassland
3) Presence of isolated large buildings (probable barns) as indicated by 1 to 5 NLCD grid cells classified as industrial/commercial within 600 meters
4) At least 1 NLCD grid cell classified as open water within 450m
5) Fewer than 6 NLCD grid cells classified as strip mines or quarries within 400 meters
6) Fewer than 30 NLCD grid cells classified as residential within 1km and less than 6 NLCD cells classified as residential within 200 meters

The NLCD land cover classification aggregates industrial, commercial, and transportation land-cover/land-use types into a single class. In order to identify areas corresponding to major transportation features (i.e., major highways) from the NLCD data, the following criteria were applied to the 30m NLCD grids:

1) Only grid cells with NLCD code 23 (commercial/industrial/transportation) were considered for inclusion
2) Not less than 25 and not more than 160 NLCD grid cells within 450 meters classified as commercial/industrial/transportation.
3) Not more than 220 NLCD grid cells within 450 meters classified as either residential or commercial/industrial/transportation.
4) At least 310 of the NLCD grid cells within 450 meters classified as forest, cropland, grassland, pasture, shrubland, or wetland.
5) Contiguous NLCD commercial/industrial/transportation grid cells must form an uninterrupted chain at least 360 meters.

Figures 3 through 7 show the relative abundance of the cropland, livestock production, residential, industrial, and transportation land-use classifications used in model development, as derived from the NLCD data sets, at 1km resolution across the CBW modeling region and surrounding areas. Land cover data from earlier 1992 NLCD release used in our previous models (Grimm and Lynch, 2007) were not included in our analyses because classifications in that release are not comparable to those in the 2001 and subsequent updates.

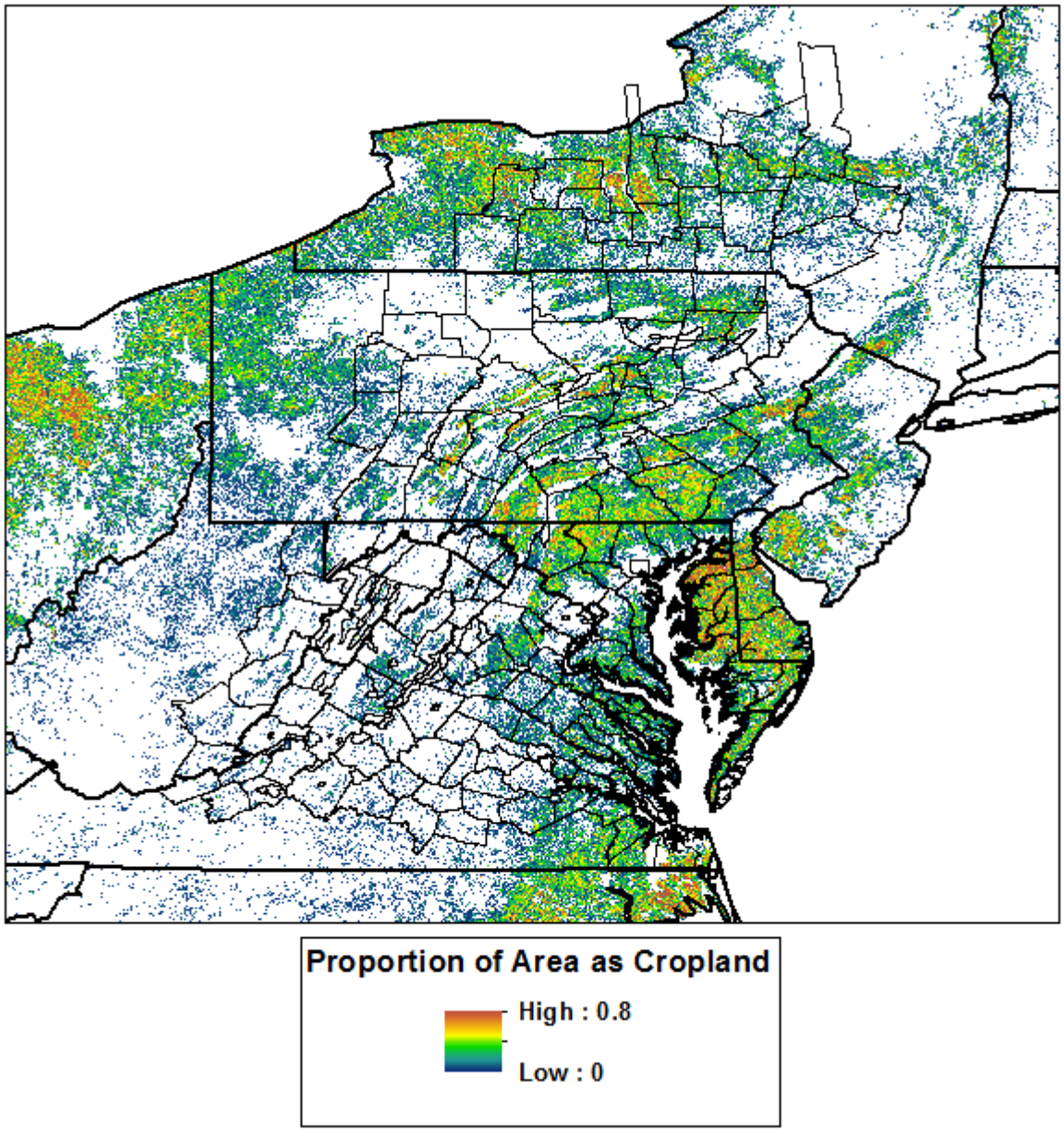

Figure 3. Proportion of land area classified as cropland as calculated from aggregation of 30-meter resolution 2011 National Land Cover Data to 1km grid cells.

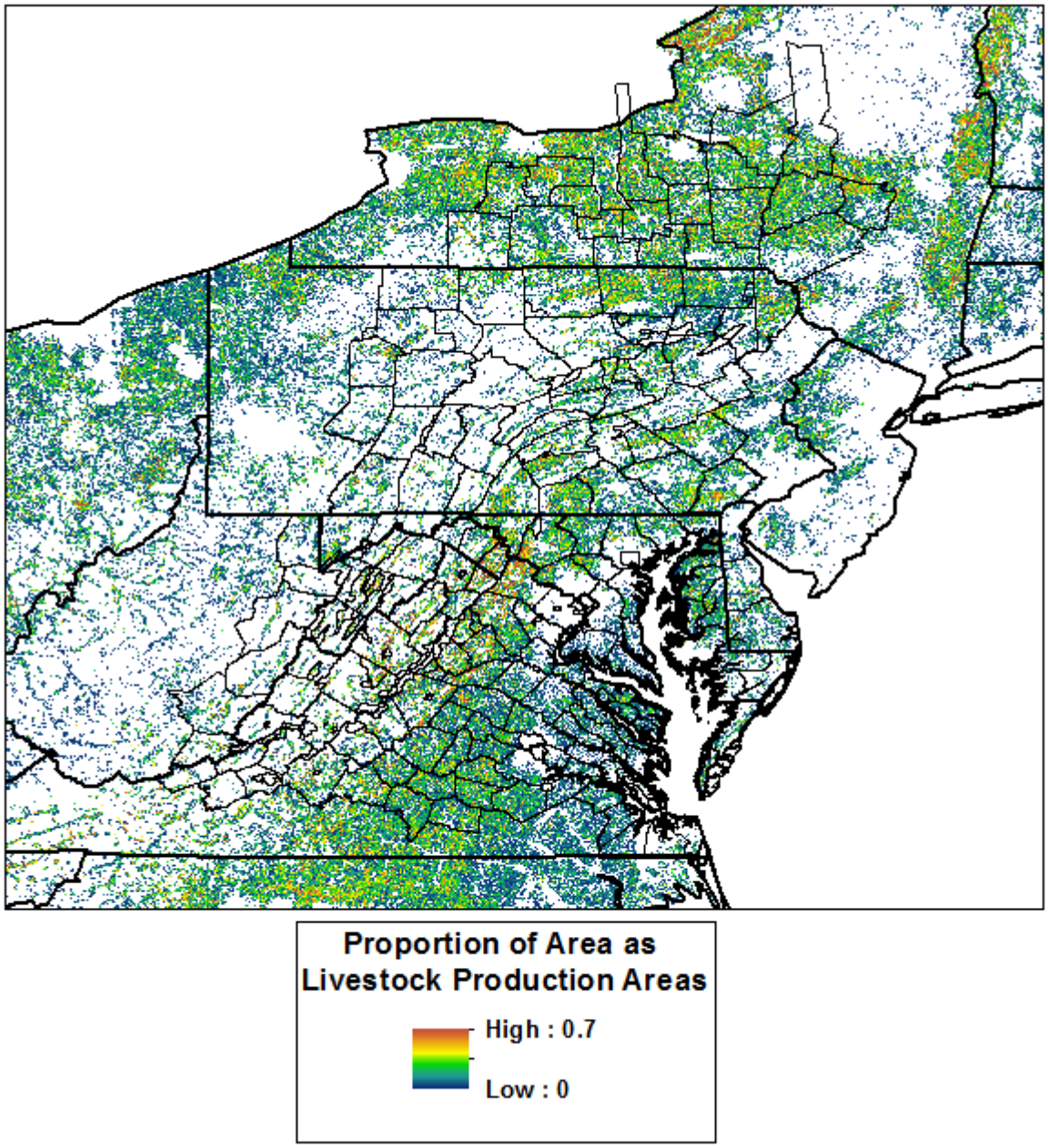

Figure 4. Proportion of land area classified as probable livestock production areas as calculated from aggregation and interpretation of 30-meter resolution 2011 National Land Cover Data to 1km grid cells.

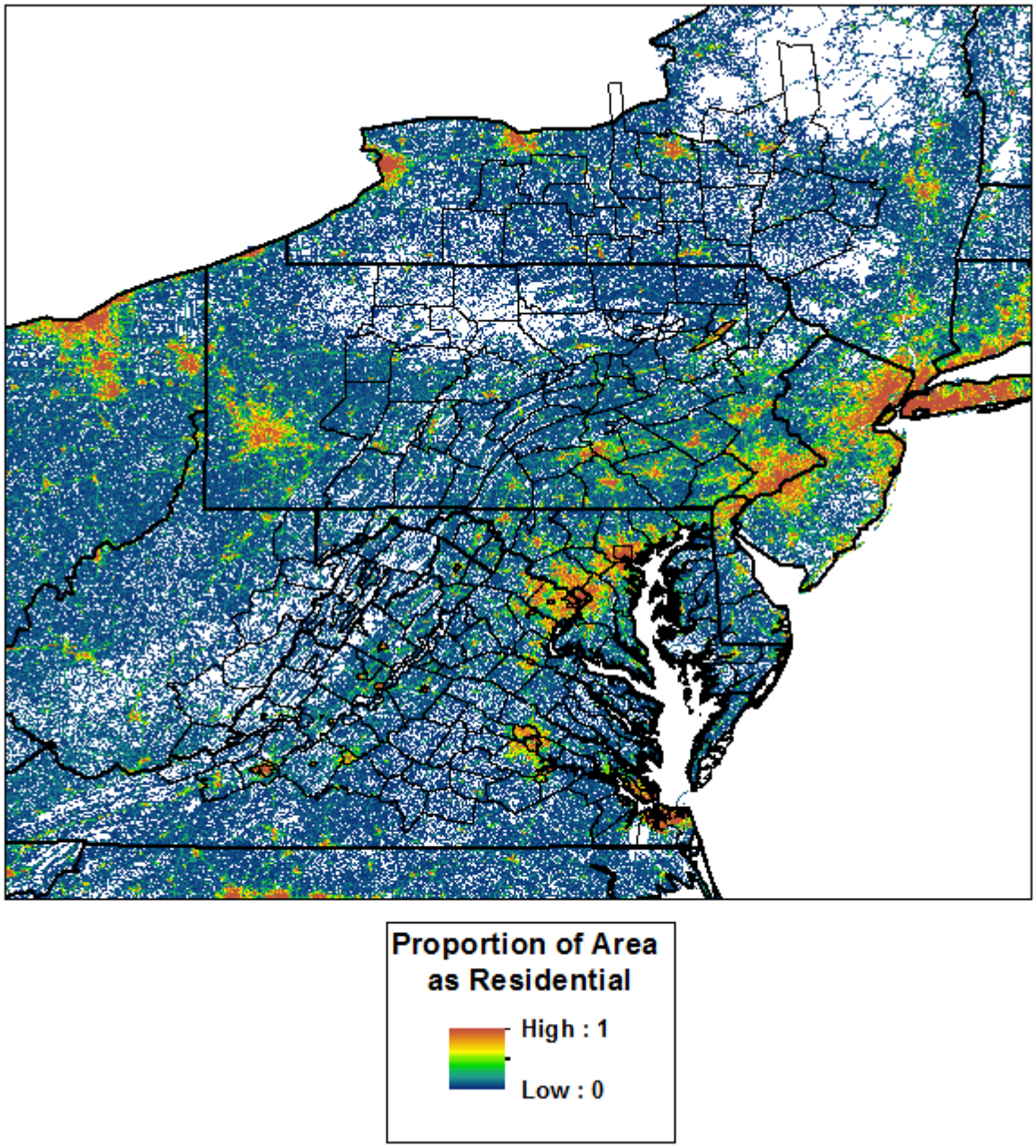

Figure 5. Proportion of land area classified as residential cover types as calculated from aggregation of 30-meter resolution 2011 National Land Cover Data to1km grid cells.

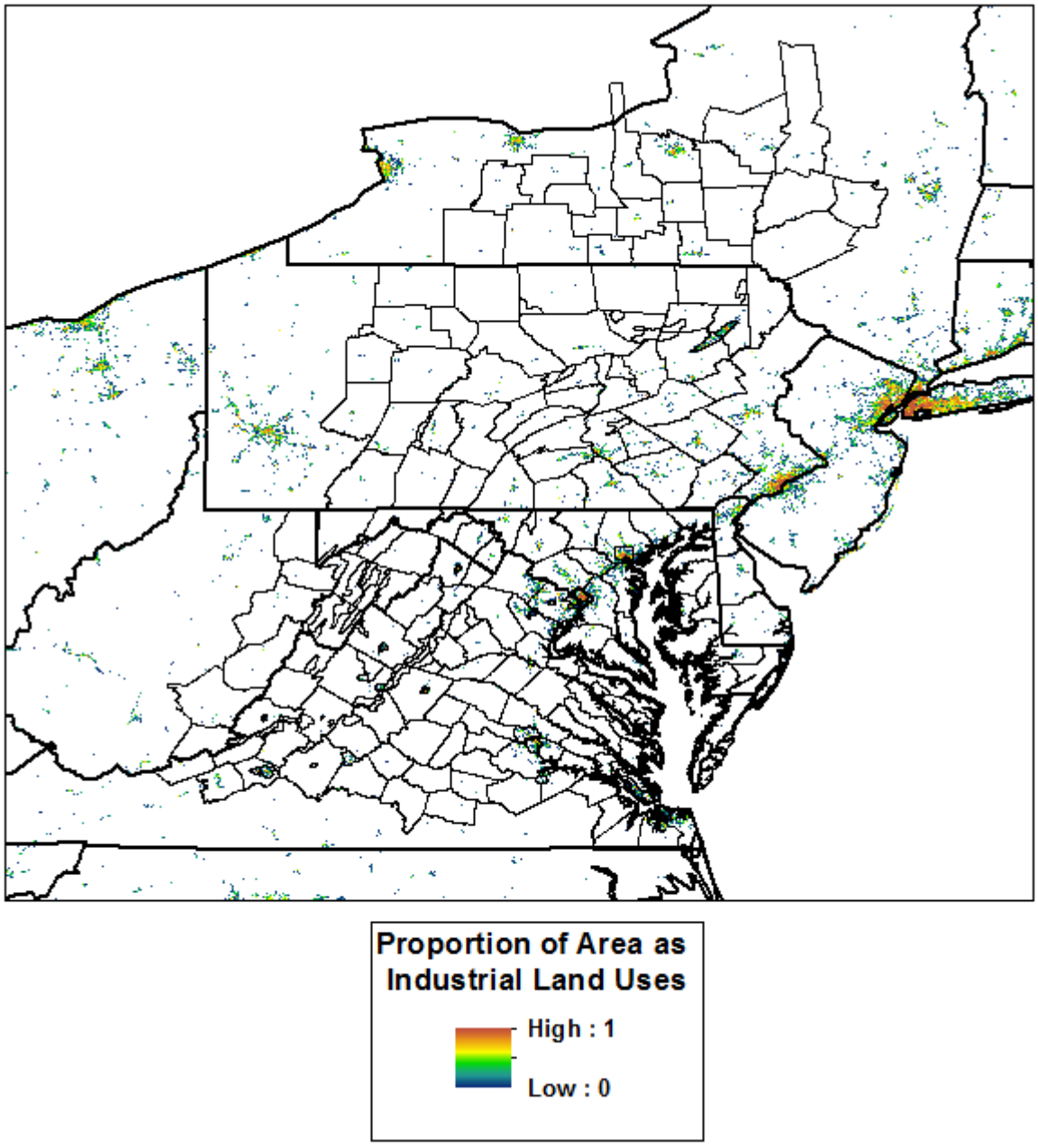

Figure 6. Proportion of land area comprised of industrial land uses as calculated from aggregation of 30-meter resolution 2011 National Land Cover Data to 1km grid cells.

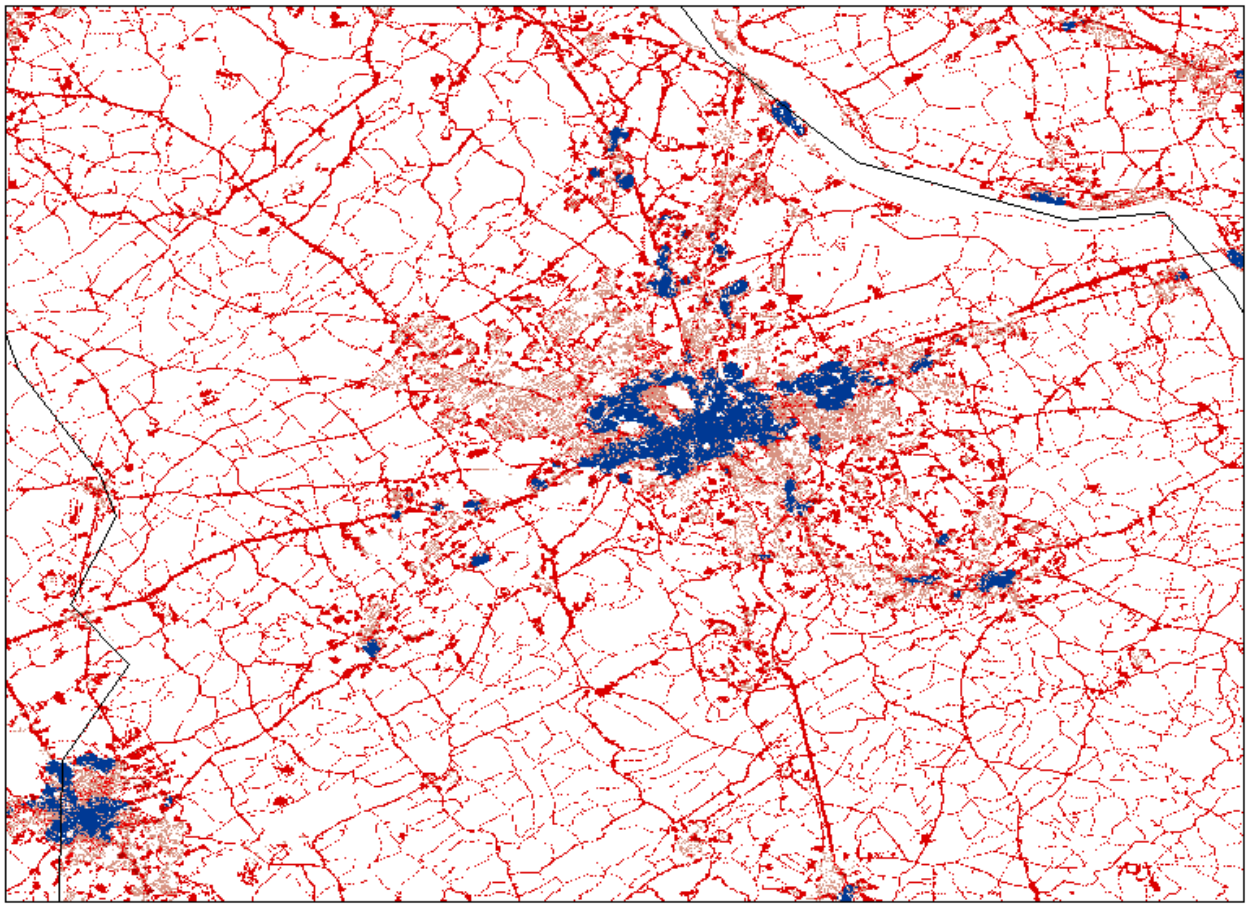

Figure 7. Classification of land area comprised of major highways as calculated from of 30-meter resolution 2011 National Land Cover Data.

Emissions Data

Local emission levels of ammonia and nitrous oxides were considered as potential predictors of ammonium and nitrate wet-fall concentrations. Emissions data were obtained from the United States Environmental Protection Agency's National Emission Inventory (NEI) database (https://www.epa.gov/air-emissions-inventories). At the time of our analyses the NEI database annual nitrous oxides and ammonia emissions totals for both individual counties and for individual facilities for years 1990, 1996, 1997, 1998, 1999, 2000, 2001, 2002, 2005, 2008, and 2011. For model development, NEI county-specific annual tier emission totals from area sources were allocated to the NLCD grid cells lying within the corresponding county based on land cover classification as follows:

NEI Ammonia Emission Tier	Assignment to Land Cover Classification
Agriculture and Forestry	Cropland (45%), Livestock Production (50%), Forest (5%)
Fuel Comb. Industrial	Industrial/Commercial (other than major highways)
Fuel Comb. Other Commercial/Institutional	Industrial/Commercial (other than major highways)
Fuel Comb. Other Residential	Residential
Other Industrial Processes	Industrial/Commercial (other than major highways)
Waste Disposal and Recycling	Industrial/Commercial (other than major highways)
Highway Vehicles	Major Highways (70%), Residential (20%), Industrial/Commercial (10%)
Off-Highway Fuel Combustion	Cropland (35%), Industrial/Commercial (50%), Strip mines (10%), Forest (5%)

NEI NOx Emission Tier	Assignment to Land Cover Classification
Fuel Combustion Other Commercial/Institutional Oil	Industrial/Commercial (other than major highways)
Fuel Combustion Other Residential	Residential
Waste Disposal and Recycling	Industrial/Commercial (other than major highways)
Highway Vehicles	Major Highways (65%), Residential (25%), Industrial/Commercial (10%)
Off-Highway Fuel Combustion	Cropland (35%), Industrial/Commercial (50%), Strip mines (10%), Forest (5%)
Miscellaneous Other Combustion	Residential (60%), Industrial/Commercial (35%), Forest (5%)

Figures 8 and 9 illustrate the allocation of NEI 2011 annual ammonia area source emissions to areas of agricultural land use and of transportation-related nitrous oxides emissions to areas corresponding to major highways and residential and industrial/commercial land uses. The NEI database also provides annual ammonia and nitrous oxide emissions from individual facility point sources. These estimates of point source emissions were incorporated into our model development by assigning the NEI specified emission level to the coordinates indicated for the corresponding facility and assuming a constant rate of emission release throughout the year. Figures 10 and 11 show the location and emission levels of ammonia and nitrous oxide from facility point sources obtained from the NEI database for the year 2011.

The NEI emissions database was selected for use in this study because it is a single, consistent source of county-specific emissions data across not only the CBW, but also across the entire spatial domain required by the emissions transport model used for Phase 6 model development. Unfortunately, the available NEI data do not cover the entire time span addressed by the current study (i.e., 1984 through 2014). The levels of ammonia and nitrous oxide emissions from other sources were defined to be the NEI values from the closest available NEI summary period.

Emissions Transport

Because nitrous oxide and ammonia emissions may potentially travel long distances between the time of release and their conversion to soluble forms and deposition in precipitation, our regression models included a number of predictors that quantify the atmospheric movements and relative concentrations of emitted nitrate and ammonium precursors. The atmospheric transport model used our model development is a simple Eulerian grid design that was operated on an hourly time-step on a 5km spatial resolution. The geographic domain for the transport model extended from 33^{o}N to 48^{o}N latitude and from 87.5^{o}W to 66^{o}W longitude. Emissions from the area and point sources described above were introduced to the atmosphere at hourly intervals from each of the NLCD grid cell centers or facility coordinates to which they were assigned based on land use classification. The rate of emission release from each source location was determined by the portion of the annual county-specific emission rate obtained from the NEI database that was allocated to that point or NLCD grid cell. Ammonia and nitrous oxide emission rates from facility point sources and from residential, industrial/commercial, forest, and strip-mine area sources were constant for each hourly release throughout a given year. Daily emission rates from individual NLCD grid cells classified as major highways were held constant throughout each year; however, hourly emission rates from these sources were determined by the following schedule:

Hour (Local Time)	Percent of Daily Emission	Hour (Local Time)	Percent of Daily Emission
00	2.45	12	4.59
01	1.53	13	4.59
02	1.53	14	4.59
03	1.53	15	4.59
04	2.14	16	7.65
05	2.14	17	7.65
06	2.14	18	7.65
07	6.42	19	3.98
08	6.42	20	3.98
09	6.42	21	3.98
10	4.59	22	2.45
11	4.59	23	2.45

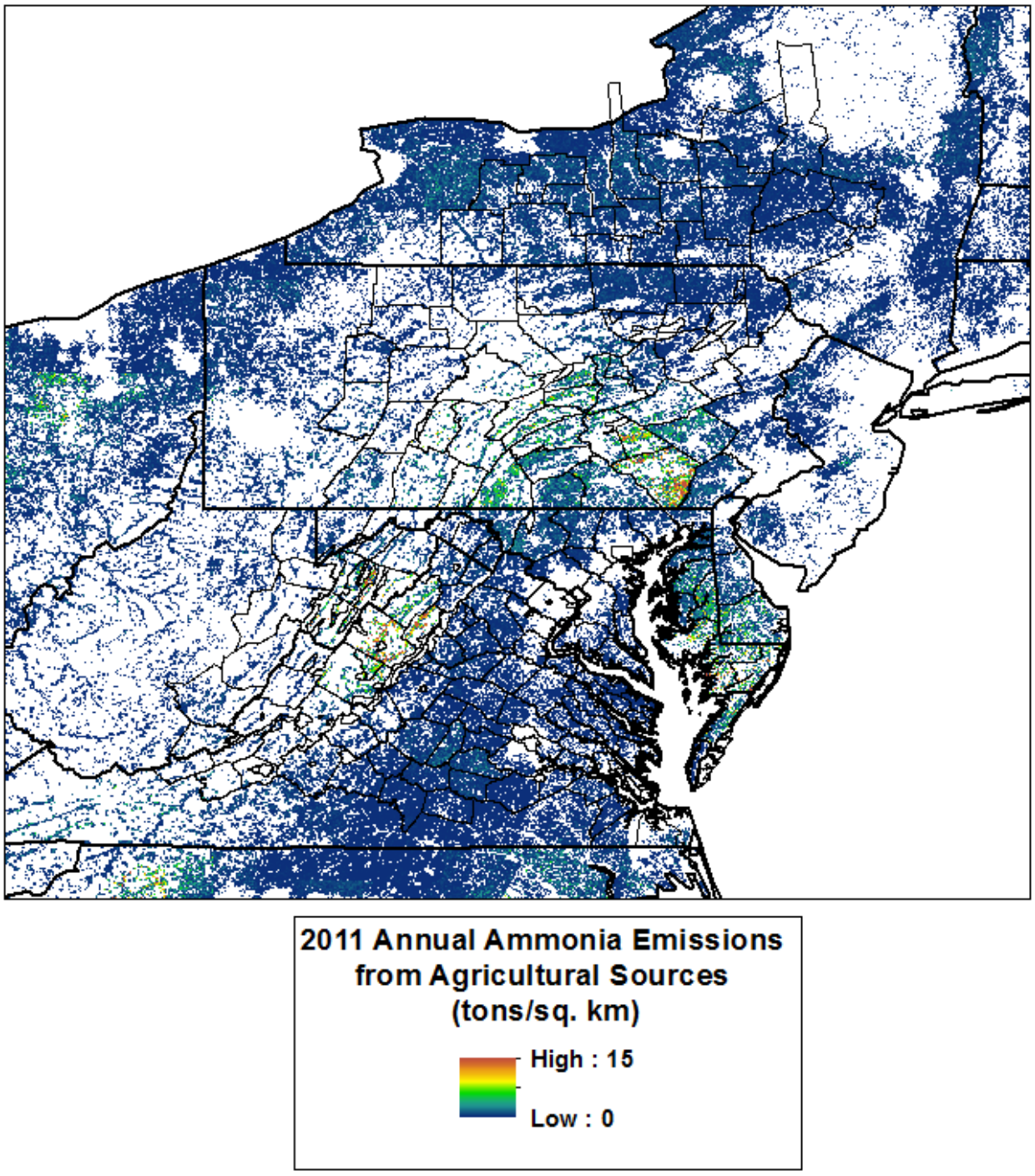

Figure 8. Allocation of 2011 annual ammonia area source emissions from the EPA National Emissions Inventory database to 2011 National Land Cover Data set grid cells that represent agricultural land uses (i.e., livestock production and cropland).

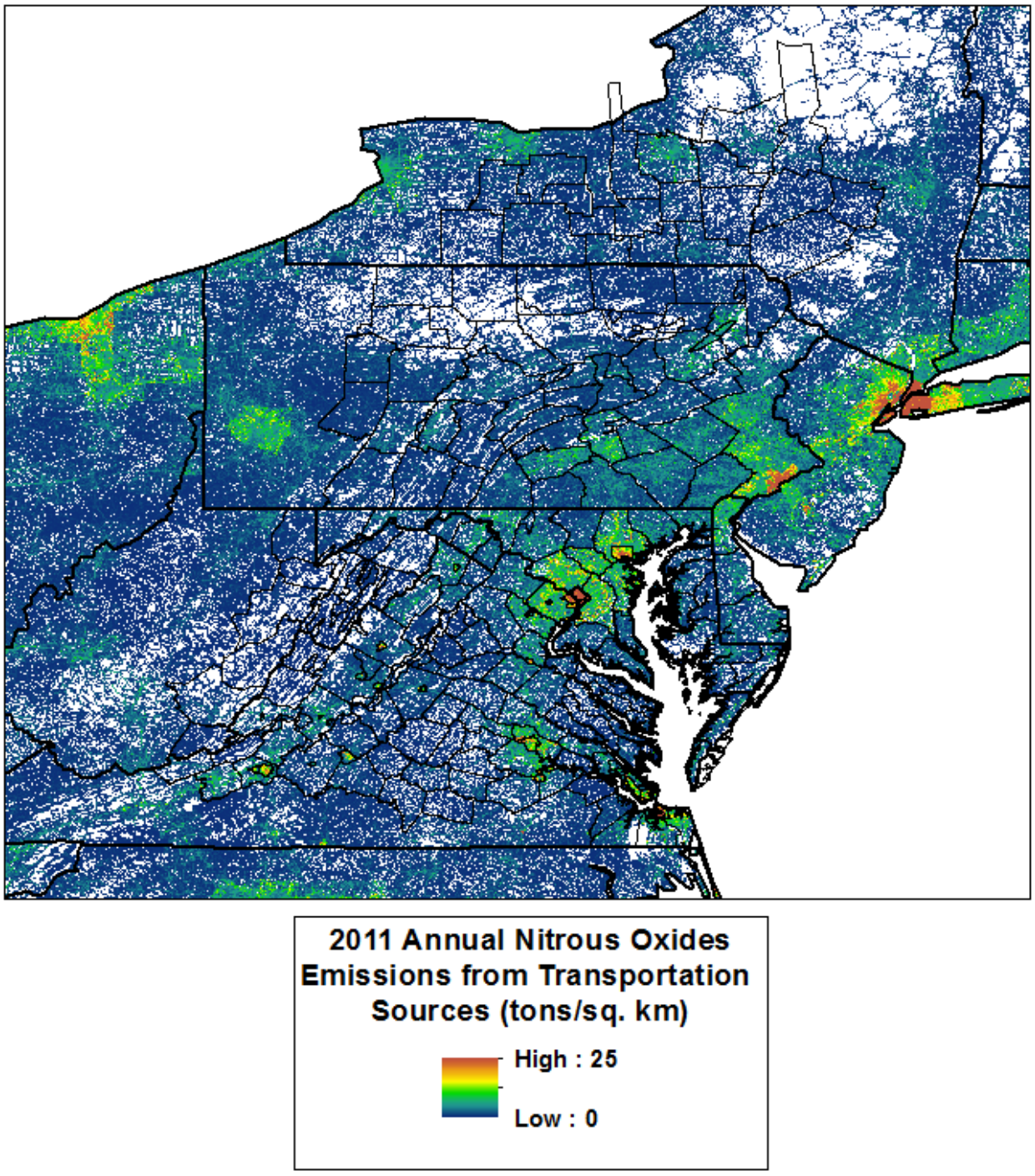

Figure 9. Allocation of 2011 transportation-related annual nitrous oxides emissions from the EPA National Emissions Inventory database to 2011 National Land Cover Data set grid cells that represent transportation, residential, and industrial/commercial land uses.

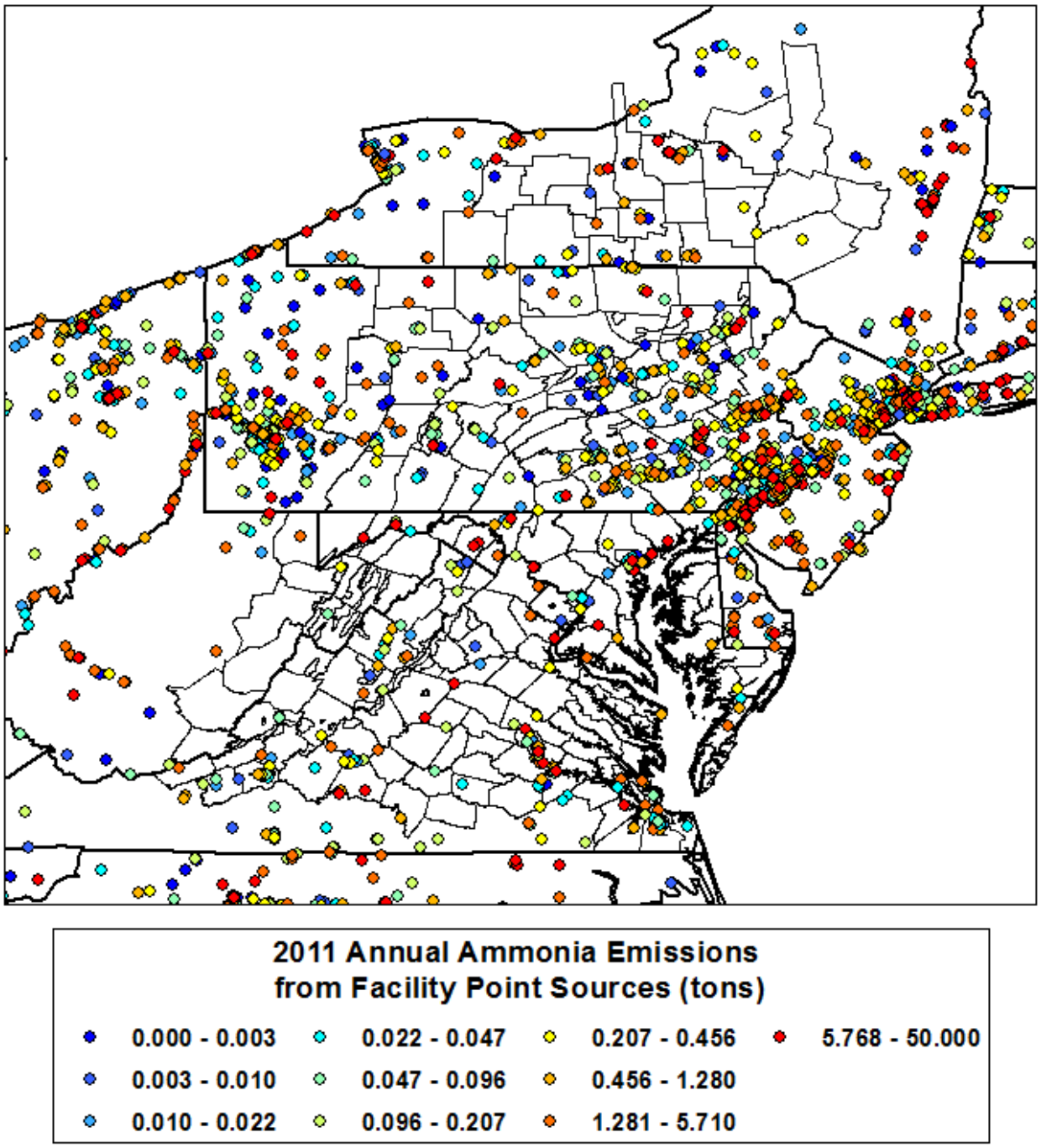

Figure 10. Location and estimated 2011 annual output of ammonia emissions from facility point sources obtained from the EPA National Emissions Inventory database.

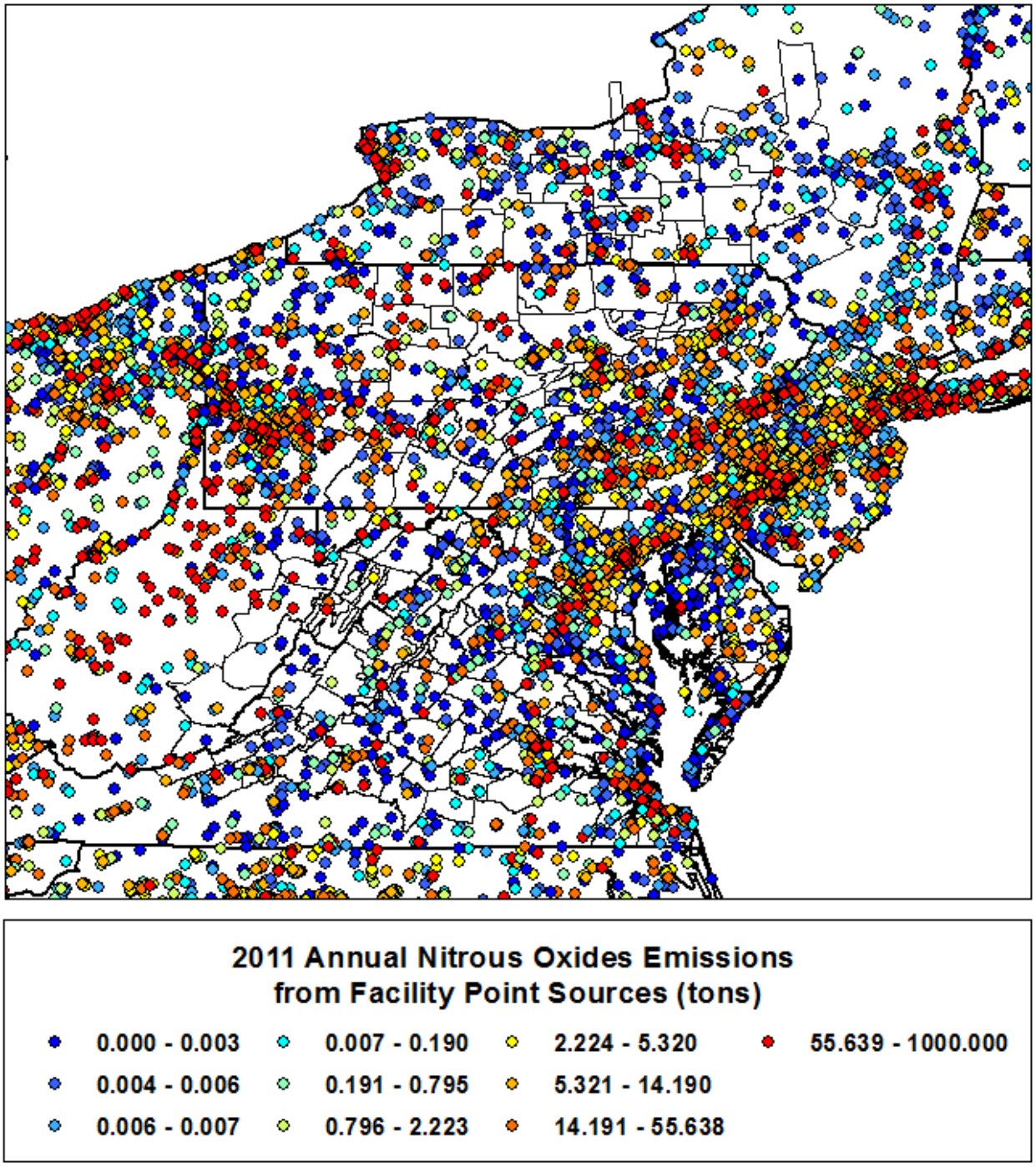

Figure 11. Location and estimated 2011 annual output of nitrous oxide emissions from facility point sources obtained from the EPA National Emissions Inventory database.

Annual total ammonia emissions allocated to NLCD grid cells classified as livestock production areas were apportioned to individual hourly release rates based the following weighting system determined by local soil temperature at 0 to 10cm depth:

Soil Temperature at 0 to 10cm Depth (^{o}C)	Hourly Weight
< 0	0.33
0 to 10	0.67
> 10	1.00

The soil temperature-derived hourly weights were normalized to an annual total of 1.0 for each location and year and then applied to the assigned annual emission rate to yield the individual hourly emissions.

Annual ammonia emissions assigned each NCLD grid cell classified as cropland were first reallocated into monthly totals according to the following schedule:

Month	Percent of Annual Emission	Month	Percent of Annual Emission
Jan	3.22	Jul	7.73
Feb	4.02	Aug	8.73
Mar	9.67	Sep	9.26
Apr	14.79	Oct	11.42
May	11.75	Nov	6.17
Jun	9.51	Dec	3.73

This monthly allocation of ammonia emissions from cropland areas reflects both a typical schedule of fertilizer application to cropland throughout the CBW modeling domain, as a whole, and the influence of soil temperatures in determining the rate at which ammonia escapes from the soil (Addiscott, 1983). Monthly ammonia emissions estimates for each NLCD grid cell were then apportioned to individual hourly emissions by applying the soil temperature weighting system described for livestock production areas above.

Meteorological data from the National Center for Environmental Prediction's North American Regional Reanalysis (NARR) model were used as inputs to the atmospheric transport model. The NARR model was selected because 1) it provides the detailed upper-air parameters required for emissions transport simulations and 2) it spans the entire time period of our modeling effort. Other surface reanalysis models, such as NLDAS-2 and RTMA provide higher-resolution data, but do not provide upper-air parameter estimates. The NARR is a reanalysis of output from the North American Mesoscale/Eta numerical weather data assimilation model to a 32-km grid for 45 vertical levels at 3-hour time intervals from 1979 through the present (Ebisuzaki, 2004). The NARR model assimilates temperature, wind, and moisture observations from surface weather stations, radiosondes, dropsondes, and aircraft and remotely-sensed measurements of cloud structure and movement to calibrate and correct short-range operational numerical weather model fields. The quality of the NARR dataset is further enhanced relative to earlier data assimilation models by the use of a refined land surface model (NOAH) and detailed terrain and vegetation databases. Although data from even higher resolution weather data assimilation programs (e.g, the RUC model at 13km resolution) are available for the most recent years, the NARR dataset represents the best long-term database available from which to draw multi-level wind movement, cloud moisture, and temperature information to incorporate into the atmospheric transport model for the CBW region for the 31-year modeling period (i.e., 1984 through 2014). In order to meet the requirements of the hourly atmospheric transport model, the 3-hourly, 32km NARR meteorological grids

were bilinearly interpolated to a 5km spatial resolution and then temporally interpolated to hourly intervals. Hourly precipitation estimates from the NLDAS-2 model were used in lieu of NARR precipitation estimates in order to standardize the precipitation measures integrated into other related modeling programs for the CBW region. NARR estimates of *u*- and *v*-component wind velocities and vertical velocities at pressure levels of 1000, 950, 900, 850, 800, 700, 600, 500mb and of surface pressure were used determine lateral and vertical movements of emissions in the transport model employed in this study. Additional NARR estimates of soil temperature and atmospheric precipitable water volume were used to model the release and wet deposition of emissions and their availability for wet deposition.

Emissions released from source locations were initially positioned at pressure altitudes indicated by the corresponding surface pressure estimate. At each hourly time step, portions of released emissions within each 5km transport model grid cell at each pressure altitude level were laterally transported along either the vector calculated from the corresponding NARR pressure-level u- and v-wind velocities or along one of 20 equal-length dispersion vectors radiating at 1-degree angular increments to either side of the central wind vector. The proportion, p_i, of emissions transported along each of the dispersion vectors was inversely related to the angular deviation from the central wind vector as follows:

$$p_i = w_i / \Sigma w_i$$

where, $w_i = \cos((\pi/2) * (|\theta_i - \theta_w| / d_{max}))$

θ_i = bearing of i^{th} vector in degrees

θ_w = bearing of central wind vector in degrees

d_{max} = maximum angular deviation from the central wind vector (20 degrees)

After each hourly lateral movement calculation, transported emissions were assumed to be uniformly distributed across the area of the destination 5km model grid cell. In transit emissions were also assumed to be uniformly distributed in the vertical direction within the current pressure altitude level. Emissions were moved between pressure altitude levels at each hourly time step according to the NARR estimate of vertical velocity at the corresponding pressure level. A maximum of 90 percent of emissions at a given pressure level were transferred to the next pressure level indicated by the direction of the vertical velocity in any single hourly time interval. In transit emissions were removed from atmospheric transport through wet deposition by precipitation at a proportional rate determined by:

$$d_h = 1 - e^{(-p_h / 31.75)}$$

where, d_h = The fraction of airborne e emissions removed during hour, *h*

p_h = The surface precipitation rate in mm/hour during hour, *h*

Only emissions at pressure altitudes of 700mb or lower were subjected to removal by wet deposition. Dry deposition losses of airborne ammonia and nitrous oxide emissions were modeled by fractionally reducing emission concentration levels within 50mb of the surface at each hourly time-step of the transport model by the following rates:

Season	Hour (local time)	Hourly Loss to Dry Deposition Percent
Ammonia Emissions:		
Growing season (15 April to 15 Oct)	08 to 19	10.0
Growing season "	00 to 07, 20 to 23	6.0
Dormant season (16 Oct. to 14 April)	00 to 23	5.0
Nitrous Oxide Emissions:		
Growing season (15 April to 15 Oct)	08 to 19	6.0
Growing season "	00 to 07, 20 to 23	1.5
Dormant season (16 Oct. to 14 April)	00 to 23	1.5

The emissions transport model was run for the entire transport domain from 21 December 1983 through 1 January 2015 for each of the following sets of emission sources derived by allocating the NEI emissions estimates to NLCD grid cells and facility coordinates:

1) Agricultural ammonia emissions - Ammonia emissions attributed to the Agriculture and Forestry emissions tier
2) Transportation ammonia emissions - Ammonia emissions attributed to the Highway Vehicle and Off-Highway Fuel Combustion emission tiers
3) Facility ammonia emissions - Ammonia emissions attributed to the facility point sources and to the Fuel Combustion Industrial, Fuel Combustion Other, and Other Industrial Processes emission tiers
4) Transportation nitrous oxide emissions - Nitrous oxide emissions allocated to the Highway Vehicle and Off-Highway Fuel Combustion emission tiers
5) Facility nitrous oxide emissions - Nitrous oxide emissions allocated to facility point sources
6) Residential nitrous oxide emissions - Nitrous oxide emission allocated to the Fuel Combustion Other Residential and Miscellaneous Other Combustion emission tiers

For each of these sets of emissions sources a series of pressure-level transported emission concentration grids spanning the 1984 through 2014 study period were generated at a 5km spatial resolution. To reduce data storage requirements, the concentration grids were summarized from the transport model's native hourly time-step to 3-hour intervals by averaging values from the constituent hourly intervals. Storage requirements were also controlled by summing individual pressure level emission concentration grids into the following categories: sub-cloud level (1000mb to 850mb), cloud level (850 to 700mb), above cloud levels (700 to 500mb).

Back-trajectory calculations using the transported emission concentration grids and NARR wind velocity and precipitation grids were performed for each single event NADP/NTN precipitation chemistry sample and for each 5km transport model grid cell location to produce the following emissions transport parameters for potential inclusion the daily wet-fall concentration regression functions:

1) Mean concentration of transported emissions along back-trajectory path at sub-cloud and cloud-levels.

2) Mean concentration of transported emissions weighted by atmospheric precipitable water at each time-step along the back-trajectory path.

Back-trajectory calculations were performed for 3-, 6-, 12-, 24-, 48-, 72-hour time spans prior to the mid-point time of each sample precipitation event. In addition to the emission concentration and loading parameters derived from the back-trajectory calculations, mean concentrations of transported emissions at sample locations during sample precipitation events were also calculated for use in development of the wet-fall concentration models.

Wet-fall Concentration Regression Model Development

Selection of wet-fall regression model effects from among the set of candidate predictors was conducted using stepwise linear least squares regression with forward selection and backward elimination of terms evaluated at each step based on a significance level of 0.05. The first step of the stepwise regression selection procedure for each ion began with event precipitation volume and seasonality included as predictors. These effects were shown to be significant predictors of both daily ammonium and nitrate wet-fall concentrations by preceding model development (Valigura et al, 1996; Grimm and Lynch, 2005). The form of the regression model used in our analysis is:

$$\log_{10}(c) = b_0 + b_1\text{sqrt}(pcp) + \Sigma b_{2s}\text{season} + b_3 v_3 + \ldots + b_n v_n + e$$

where,

	c	=	event wet-fall ionic concentration (mg/L)
	b_0	=	intercept
	pcp	=	event precipitation volume (inches)
	b_1	=	coefficient for precipitation term
	season	=	vector of 5 binary indicator variables encoding the 6 bi-monthly seasons
	b_{2s}	=	vector of 5 coefficients for seasonal terms
	$v_3 \ldots v_n$	=	additional predictors selected through stepwise regression
	$b_3 \ldots b_n$	=	coefficients corresponding to $v_3 \ldots v_n$
	e	=	residual error

Log_{10} or square root transformations of individual predictors, v_i, were performed to stabilize the variance of model residuals, improve normality of residual distributions, and to optimize fit of the regression models.

Model Verification

The wet-fall concentration models obtained through the stepwise regression process were verified by comparing model estimates of wet deposition with single event and annual wet depositions reported at 36 of the NADP/NTN and PADM monitoring sites within the CBW modeling region that have 10 or more years of precipitation chemistry data which met the completeness criteria. Model estimates used for verification comparisons with NADP/NTN observations were produced by withholding the data for a single, selected monitoring site within a selected year, fitting the regression model with the predictors chosen by the stepwise regression procedure described early, and then calculating the estimates for that site location for the precipitation events occurring during the given year. The process of generating model estimates while withholding data for combinations of individual monitoring site and year was repeated until estimates for all combinations of site and year were obtained.

Estimates of daily or event ionic wet deposition were calculated as the product of estimated concentration and precipitation volume as follows:

$$d = 0.254 * c * pcp$$

where, d = estimated daily or event ionic wet deposition (kg/ha)
c = estimated daily or event ionic wet-fall concentration (mg/L)
pcp = daily or event precipitation volume (inches)

Estimates of daily ammonium, nitrate, and inorganic nitrogen wet deposition rates (kg/ha/day) to the land modeling segments and the water quality management (WQM) cells employed by the Phase 6 Watershed Modeling Program for the CBW were calculated by first estimating daily deposition rates within the cells of a uniform 5km grid overlaying the CBW modeling region and then calculating an area-weighted mean the deposition for each land modeling segment or WQM unit polygon based on its area of intersection with the individual 5km grid cell rectangles. Precipitation volumes from the NLDAS-2 surface precipitation grids were used to calculate estimated wet depositions for both the land modeling segments and WQM cells and for verification of model performance relative to single-event and annual deposition rates reported at NADP/NTN and PADM stations.

Long-term Trends of Estimated Wet Deposition

Long-term trend models of annual ammonium nitrogen, nitrate nitrogen, and total inorganic nitrate wet deposition, as estimated by combined concentration estimates from the Phase 6 ammonium and nitrate wet-fall concentration models with estimates of precipitation from the NLDAS-2 model, were calculated for each Phase 6 land segment and water quality model cell by linear least squares regression. The fitted annual trend regression model is of following form:

$$\log_{10}(N_{dep}) = b_0 + b_1 * year_{adj} + b_2 * sqrt(year_{adj})$$

or, alternatively,

$$N_{dep} = 10.0 \wedge (b_0 + b_1 * year_{adj} + b_2 * sqrt(year_{adj}))$$

Where,

N_{dep} = estimated annual wet deposition of nitrogen in lb/acre for land segments and kg/ha for water quality model cells
$year_{base}$ = year baseline model parameter
$year_{adj}$ = year to be estimated - $year_{base}$ model parameter (e.g., 2016 – 1978 = 38)
b_0 = intercept coefficient
b_1 = slope coefficient for the $year_{adj}$ model predictor
b_2 = slope coefficient for the sqrt($year_{adj}$) model predictor

Values for $year_{base}$, b_0, b_1, and b_2 for each Phase 6 land segment or water quality model cell were provided to the Chesapeake Bay Program for use in additional simulations. Regression model parameters for Phase 6 land segments were indexed by their FIPSNHL polygon attribute. Model parameters for water quality model cells were indexed by their WQMCELLID attribute (and HYDROID attributes for cells with WQMCELLIDs of 0).

Results and Discussion

Ammonium Wet-Fall Concentration and Wet Deposition

Model Development

The regression model developed to predict daily ammonia wet-fall concentration from temporal and geographic parameters, rainfall volume and chronology, land use characteristics, and estimated distributions of ammonia emissions is detailed in Table 2. The resultant regression model indicates that a large subset of the available predictors jointly and significantly contribute to the estimation of wet-fall ammonium concentrations across the CBW modeling domain and that overall patterns are dominated by measures of seasonality. Although no evidence of multi-collinearity was found amount the selected predictors, the model's parameter estimates must be interpreted jointly as the predictors are not completely orthogonal. The parameter estimates for individual predictors in a multiple regression model of inter-correlated covariates are conditional on the other predictors in model and do not represent the simple bivariate relationship between the individual predictors and the dependent variable. These constraints on interpretation of parameter estimates particularly apply to the long-term trends induced by the year covariates. In order to clarify the long-term trends implied by the ammonium wet-fall concentration model, statistical and graphical summaries of trends in the model estimates will be presented later in this report.

In spite of the interdependencies of the covariates of the ammonium wet-fall concentration regression model, the influence and relative importance of most of the predictors can be inferred. An inverse relationship between event precipitation volume and wet-fall ammonium concentrations at NADP/NTN sites was quite apparent (Fig. 13); and, as indicated by the corresponding conditional sums-of-squares, is the most influential effect in the regression model after factoring in bimonthly seasonal variation. A modest, but significant inverse relationship between the volume of precipitation falling in the 24 hours prior to a precipitation event was also evident.

Our regression analyses resulted in the inclusion of a number of land use and emissions concentration parameters in the ammonium well-fall concentration model that represent anthropogenic influences and were all positively associated with increasing ammonium concentration estimates. The local prevalence of livestock production, cropland cultivation, and associated ammonia emissions and corresponded to elevated ammonium concentration estimates with the influence of emissions from livestock production being most pronounced. Ammonia emissions from agricultural sources area can be expected to follow the a seasonal pattern resulting from the application of manure and ammonia-containing fertilizer to croplands during the spring and during the summer months when soil temperatures are highest. The local prevalence of high intensity residential development and transportation corridors also significantly contributed to estimated ammonium wet-fall concentrations. Although the contribution to the overall model fit by residential development and transportation factors are relatively minor, it should be noted that these land use types are limited in spatial extent across the modeled domain and are not heavily represented by the NADP/NTN monitoring locations that provided the sample data used in our analyses. A significant latitudinal gradient in reported ammonium wet-fall concentrations persisted after accounting for seasonality, precipitation volume, land use, and emissions factors. This latitudinal gradient may at least partially reflect the lack of land use and emissions data for portions of southern Ontario adjoining the modeled domain.

Table 2. Linear least-squares model of daily ammonium (NH_4^+) wet-fall concentration for the Chesapeake Bay modeling region for developed from measures of long-term trend, seasonality, spatial location, precipitation volume, precipitation event history, land-use composition, and both transported emissions and static spatial distributions of ammonia emissions sources. The temporal scope of the model is from 1984 through 2014.

Dependent Variable: log10([NH4-(mg/L)])
Number of observations: 13,740 Model r2: 0.4059

Predictor	Coefficient	DF	Type III Sum of Squares	p
intercept	-1.64642			<0.0001
event precipitation (inches)	0.10827	1	9.522	<0.0001
sqrt(event precipitation (inches))	-0.73862	1	92.174	<0.0001
24hr antecedent precipitation (inches)	-0.16527	1	4.177	<0.0001
event date - 1977 (as decimal year)	0.00227	1	2.807	<0.0001
CAAA 1990 indicator (0 before 1990;1 after 1990)	0.10880	1	8.486	<0.0001
cool season (1 during September through February, 0 during March through August)	-0.07119	1	3.053	<0.0001
bimonthly season of event (6 categorical levels)		5	212.987	<0.0001
jan-feb	0.02073			
mar-apr	0.27924			
may-jun	0.38368			
jul-aug	0.34623			
sep-oct	0.07014			
nov-dec	0.00000			

Table 2 (continued).

Predictor	Coefficient	DF	Type III Sum of Squares	p
sqrt(crop land use within 64km (inverse distance-weighted relative fraction))	0.23702	1	17.800	<0.0001
sqrt(livestock production land use within 64km inverse distance-weighted relative fraction))	0.26029	1	4.818	<0.0001
sqrt(mean concentration of transported livestock emissions during 24-hour back-trajectory (weighted by atmospheric precipitable water))	0.01161	1	28.882	<0.0001
log10(mean concentration of transported livestock emissions during 3-hour back-trajectory))	0.05285	1	5.556	<0.0001
sqrt(heavy residential land use within 48km (inverse distance-weighted relative fraction))	0.30885	1	3.008	<0.0001
transportation land use within 64km (inverse distance-weighted relative fraction)	0.98407	1	3.793	<0.0001
latitude (degrees)	0.02063	1	26.900	<0.0001

The overall fit of the ammonium wet-fall concentration model for the period spanning 1984 through 2014 (Fig. 12, r^2=0.4059) is an improvement over that developed for NADP/NTN samples collected in and around the CBW modeling region during 1984 through 2001 (r^2=0.3148; Grimm and Lynch, 2005) and a slight reduction in fit to the model developed in our Phase 5 analyses for the sample period 1984 through 2005 (r^2=0.4763; Grimm and Lynch, 2007). However, the current Phase 6 model not only encompasses an extended span of years, but also describes ammonium concentrations at a much larger set of sampling sites (39 vs 85) representing a wider variety of land use patterns and anthropogenic influences; and, therefore, addresses a more heterogeneous set of environments. The Phase 6 model also incorporated fewer predictors that the previous Phase 5 model (14 vs. 27). The Phase 6 model identified no important interactions between seasonality and the individual precipitation, land use, and emissions covariates. This contrasts with the Phase 5 model which included 8 significant, but relatively weak, interactions between seasonality and precipitation, land use, and emissions predictors. Given the smaller sample set used in the Phase 5 analyses and the more restricted range environmental settings represented by those data, it is possible that the earlier Phase 5 model was somewhat over-fit and less robust than the revised Phase 6 model.

Model Verification

Comparison of estimates of single event ammonium nitrogen wet deposition derived from the Phase 6 ammonium wet-fall concentration model and precipitation volumes from the NLDAS-2 with reported daily, single event depositions at the 36 NADP/NTN sites within the CBW region that were active for at least 10 years from 1984 through 2014 (Table 3) indicates that the Phase 6 model underestimated the reported event ammonium wet depositions at those sites with a mean bias of -0.95 percent (range: -3.55 percent at WV04 to -0.03 percent at WV05). Correlations between the Phase 6 model estimates of single event ammonium wet deposition and the reported rates at the 36 NADP/NTN sites ranged from 0.4620 at TN04 to 0.7388 at MD03 with a mean correlation of 0.6072.

The mean percent absolute difference between annual ammonium nitrogen wet depositions reported by the 36 NADP/NTN sites in the CBW region during 1984 through 2014 (Table 4) and the estimates from the Phase 6 ammonium model (2.49 percent) represents a substantial improvement over the 19.0 percent rate obtained from our initial ammonium concentration model (Grimm and Lynch, 2005) and the 6.01 percent mean absolute error from the Phase 5 model (Grimm and Lynch, 2007). The mean bias of annual ammonium wet deposition estimates at the 36 long-term NADP/NTN sites for the Phase 6 model is 0.44 percent. The mean temporal correlation between annual wet deposition estimates from the Phase 6 ammonium model and annual ammonium wet deposition records from the 36 long-term NADP/NTN stations was 0.9325. We believe degree of spatial and temporal agreement between reported annual ammonium depositions and the Phase 6 model estimates is adequate to allow use of the model to describe spatial patterns and long-term trends in ammonium wet deposition throughout the CBW modeling domain during 1984 through 2014.

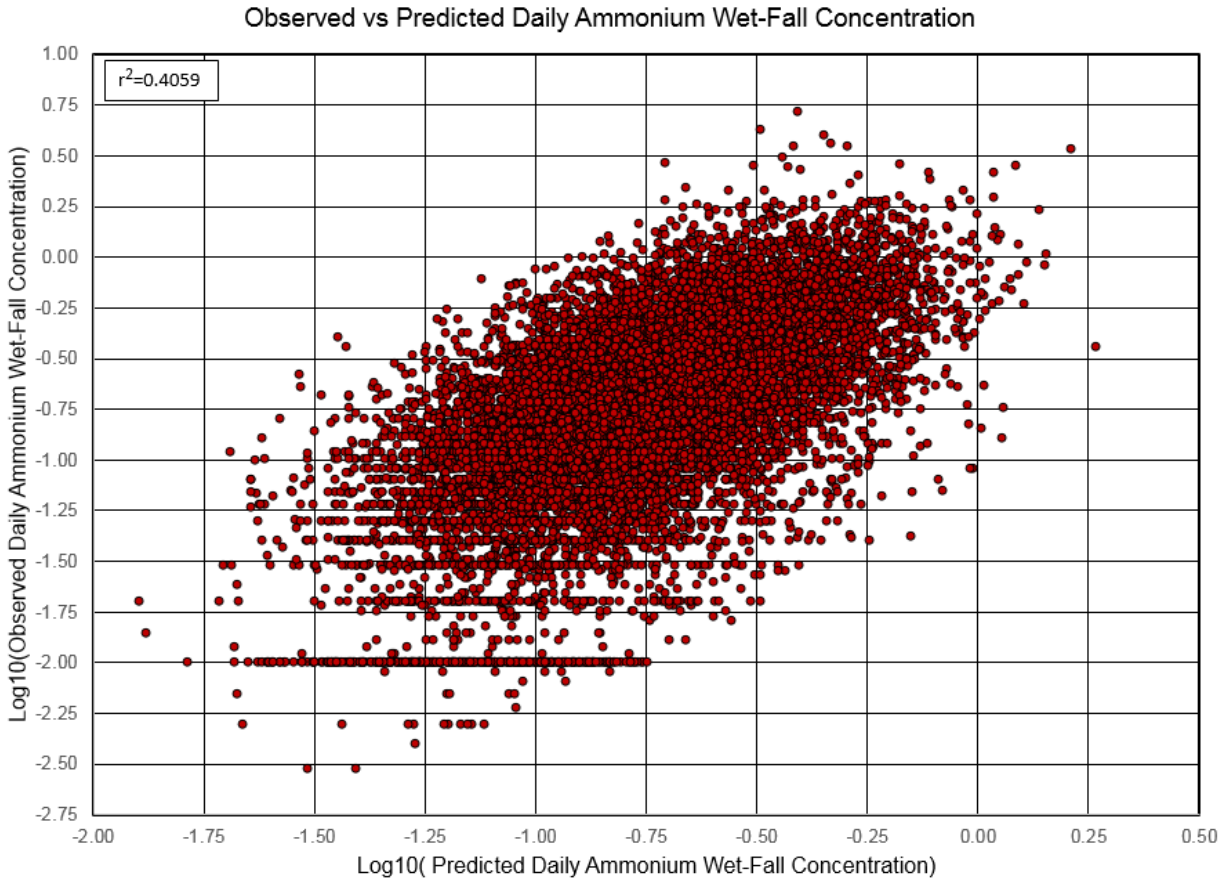

Figure 12. Comparison of estimates from the Phase 6 daily ammonium (NH_4^+) wet-fall concentration model to reported measurements of ammonium concentration in single event precipitation samples collected at 85 NADP/NTN and PADM sites in the Chesapeake Bay Watershed modeling domain region during 1984-2014.

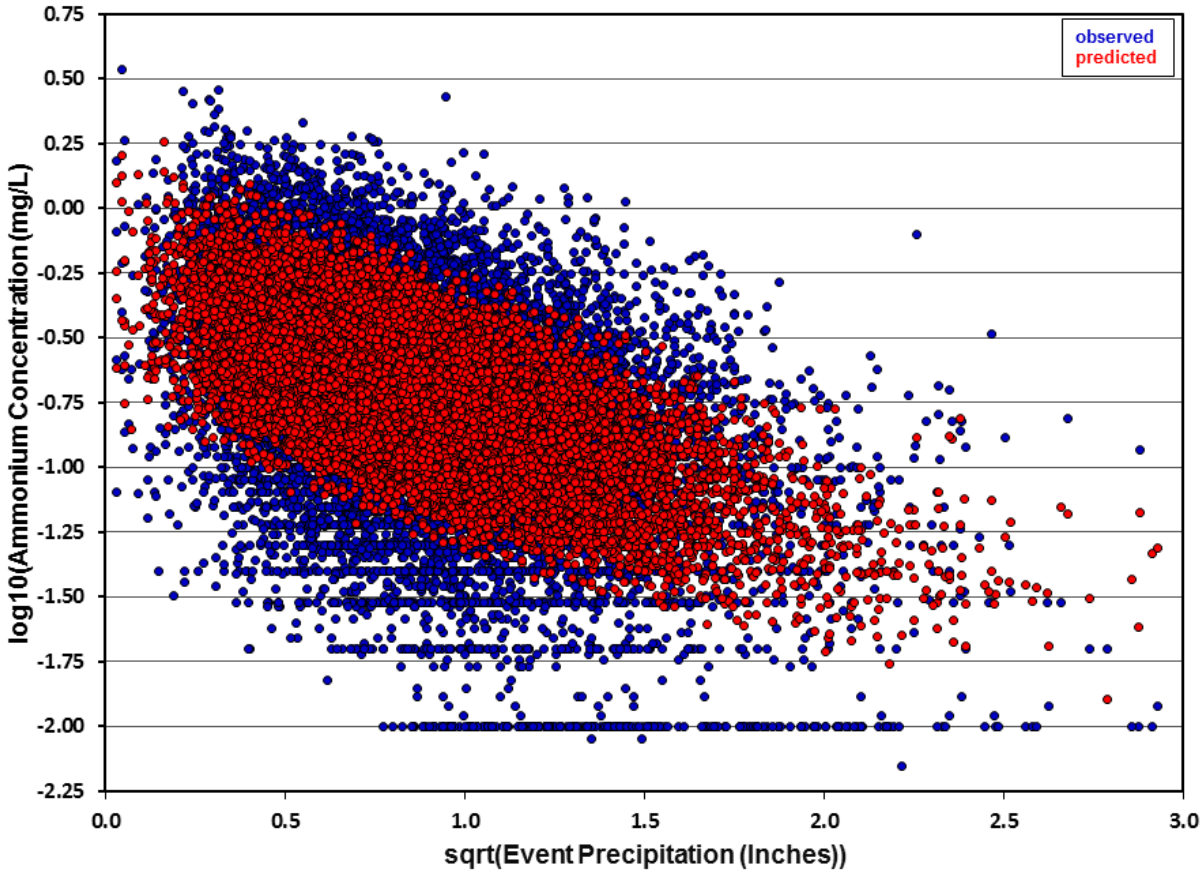

Figure 13. Relationship of observed single-event ammonium (NH_4^+) wet-fall concentrations at 85 NADP/NTN sites in the Chesapeake Bay Watershed region during 1984-2014 and estimates from the Phase 6 daily ammonium wet-fall concentration models to precipitation event volume from the NLDAS-2 model.

Table 3. Comparison of single event ammonium nitrogen (NH_4-N) wet depositions recorded at long-term 36 NADP/NTN sites located within or adjacent to the CBW region with estimates derived from the Phase 6 ammonium wet-fall concentration model and NLDAS-2 precipitation volumes. Observations for the NADP/NTN sites spanned 1984 through 2014.

Site	Number of Events	Mean Percent Error	Mean Absolute Percent Error	Correlation
KY22	236	-1.61	8.08	0.4867
MD03	135	-0.83	7.00	0.7388
MD08	61	0.99	7.00	0.6583
MD13	257	-0.81	7.14	0.6455
NC03	265	-0.34	7.69	0.6198
NC34	242	-1.10	7.09	0.6113
NC41	288	-0.22	6.84	0.5873
NJ99	308	-1.46	7.67	0.5151
NY08	136	-1.33	7.29	0.6208
NY10	122	-2.10	7.06	0.5964
NY20	126	-1.18	7.94	0.5324
NY22	73	-0.74	7.41	0.6953
NY29	53	-1.01	7.57	0.7193
NY52	101	0.20	7.28	0.5049
NY65	95	-0.18	7.60	0.7071
NY68	248	-1.02	8.10	0.4892
NY98	108	1.28	7.56	0.7283
NY99	308	-2.31	7.78	0.5524
OH49	204	-1.07	7.46	0.5695
OH71	208	0.85	6.73	0.6753
PA00	170	-0.57	7.10	0.6448
PA15	267	-1.20	7.39	0.5635
PA18	149	-1.29	7.35	0.6109
PA29	161	-1.24	7.76	0.5930
PA42	243	-0.07	7.44	0.5802
PA72	255	-1.83	7.72	0.4937
TN00	226	-1.45	7.47	0.6671
TN04	143	-1.58	6.93	0.7013
TN11	209	-0.11	8.21	0.4620
VA00	242	-1.60	7.56	0.4856
VA13	185	-1.94	7.77	0.6329
VA24	153	-1.03	7.31	0.6669
VA28	262	-1.62	7.73	0.6114
WV04	129	-3.55	8.32	0.5520
WV05	91	-0.03	7.62	0.7081
WV18	154	-1.27	8.24	0.6328
Mean		-0.95	7.51	0.6072

Table 4. Comparison of annual ammonium nitrogen (NH_4-N) wet depositions recorded at long-term 36 NADP/NTN sites located within or adjacent to the CBW region with estimates derived from the Phase 6 ammonium wet-fall concentration model and NLDAS-2 precipitation volumes. Observations for the NADP/NTN sites spanned 1984 through 2014.

Site	Number of Years	Mean Observed Deposition ------ kg N/ha	Mean Estimated Deposition --------	Mean Percent Error	Mean Absolute Percent Error	Temporal Correl.
KY22	31	1.6527	1.6544	0.37	2.02	0.9393
MD03	16	2.0509	2.0523	0.15	2.12	0.9579
MD08	10	1.4947	1.5504	4.33	4.33	0.8433
MD13	30	1.9702	1.9613	-0.36	1.52	0.9493
NC03	31	1.8844	1.8957	0.91	1.97	0.8973
NC34	30	2.4698	2.5110	1.95	2.90	0.9159
NC41	28	2.7471	2.7695	0.76	1.36	0.9763
NJ99	30	2.1100	2.1465	1.93	4.43	0.8861
NY08	31	2.6832	2.6845	0.19	1.63	0.9545
NY10	18	2.9416	2.9611	0.73	1.91	0.9286
NY20	30	1.6130	1.5908	-1.41	2.50	0.9123
NY22	12	2.1910	2.1888	-0.15	1.62	0.9456
NY29	11	2.0916	2.1123	1.03	1.60	0.9349
NY52	23	3.6232	3.6364	0.49	2.69	0.9150
NY65	17	1.5877	1.5948	0.67	1.74	0.9319
NY68	28	2.1797	2.1627	-0.59	3.21	0.9240
NY98	27	1.8092	1.7993	-0.27	2.44	0.9366
NY99	28	2.1035	2.1539	2.29	3.71	0.8906
OH49	30	2.3321	2.3357	0.23	2.42	0.9690
OH71	31	2.8658	2.8739	0.39	1.26	0.9960
PA00	15	3.0739	3.0960	1.09	2.71	0.9576
PA15	30	2.1574	2.2041	2.38	3.84	0.9010
PA18	14	2.0965	2.0988	0.56	2.61	0.9431
PA29	48	2.5084	2.4809	-1.01	3.01	0.9189
PA42	30	2.2674	2.2934	1.24	2.51	0.9443
PA72	24	1.9231	1.9605	1.39	3.72	0.9255
TN00	25	1.9757	1.9911	1.02	1.81	0.9721
TN04	15	2.0608	2.0452	-0.69	1.47	0.9690
TN11	29	2.0044	1.9665	-1.70	2.80	0.9367
VA00	24	1.9758	1.9638	-0.45	3.28	0.9374
VA13	23	1.5655	1.5630	-0.01	1.65	0.9301
VA24	15	1.6327	1.6036	-0.92	3.66	0.8970
VA28	21	2.2418	2.2112	-1.37	2.37	0.9256
WV04	19	1.8746	1.8613	-0.69	2.41	0.9383
WV05	14	1.7094	1.7430	1.69	2.73	0.9271
WV18	30	2.1887	2.1770	-0.45	1.78	0.9423
Mean		2.1571	2.1637	0.44	2.49	0.9325

Spatial Patterns and Temporal Trends in Ammonium Wet-Fall Concentration and Wet Deposition

The composite effects of the seasonal, land use, and emissions transport and intensity parameters in the Phase 6 ammonium wet-fall concentration model are illustrated by the color-scaled mapping of mean seasonal concentration estimates during the last 7 years of the modeling period (Figure 14). A seasonal cycle in estimated ammonium concentration is quite evident with levels rising abruptly throughout the Chesapeake Bay region during the early spring, peaking in late late-spring, and remaining elevated throughout the mid-summer before sharply falling in early autumn. In spite of the strong precipitation volume dilution effect in the model, the highest concentrations are indicated during the months with the greatest precipitation and are concurrent with seasons of peak crop production activities. The most distinctive features in the ammonium concentration maps are the spatially limited, but sharply elevated estimates in areas with heavy residential development and transportation land uses. Another less dramatic, but much more widespread, pattern that is apparent in all seasonal concentration maps is that of elevated estimates in areas with increased agricultural ammonia emissions (see Fig. 8) and livestock and crop production.

Mapping of mean annual volume-weighted ammonium concentration estimates from the Phase 6 model doesn't reveal an overall pattern of consistently increasing or decreasing levels throughout the Chesapeake Bay region over the span of the modeling period (Fig. 15). There is an indication of a general increase in concentration across the southern third of the modeled domain particularly from south-central Virginia northeastward through Delaware. Estimates of seasonal and annual ammonium wet deposition produced by combining the Phase 6 models concentration estimates with precipitation volume estimates from the NLDAS-2 model (Figs. 16 and 18) correspond well with the mapping of the model's concentration estimates (Figs. 14 and 15) and reflect similar patterns of change during the modeling period. Spatial patterns of precipitation within seasons (Fig. 17) are not strongly to corresponding spatial patterns of ammonium wet deposition (Fig. 16).

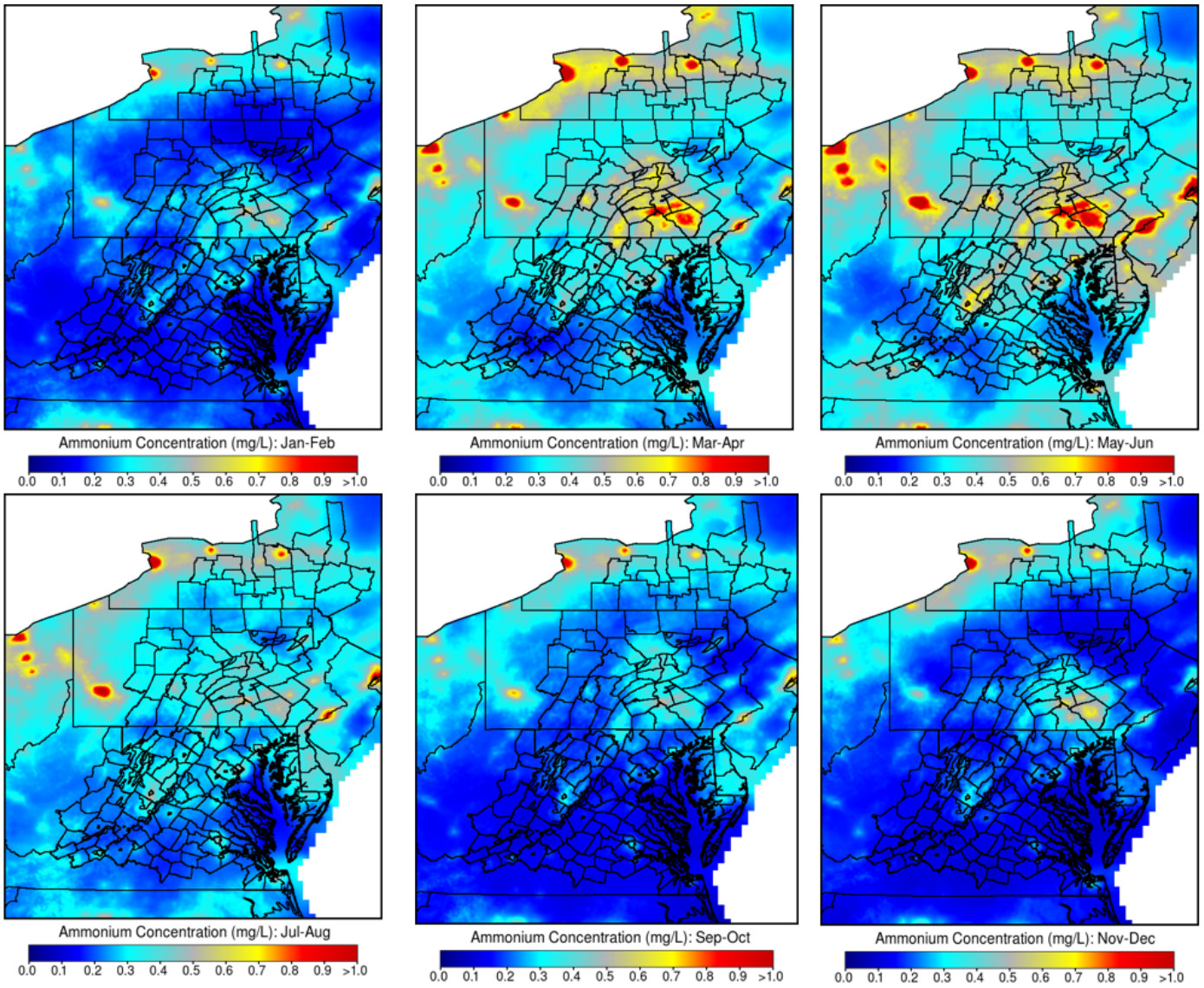

Figure 14. Seasonal mean ammonium (NH_4) wet-fall concentrations across the Chesapeake Bay Watershed region during 2010-2014 as estimated by the Phase 6 daily ammonium wet-fall concentration model.

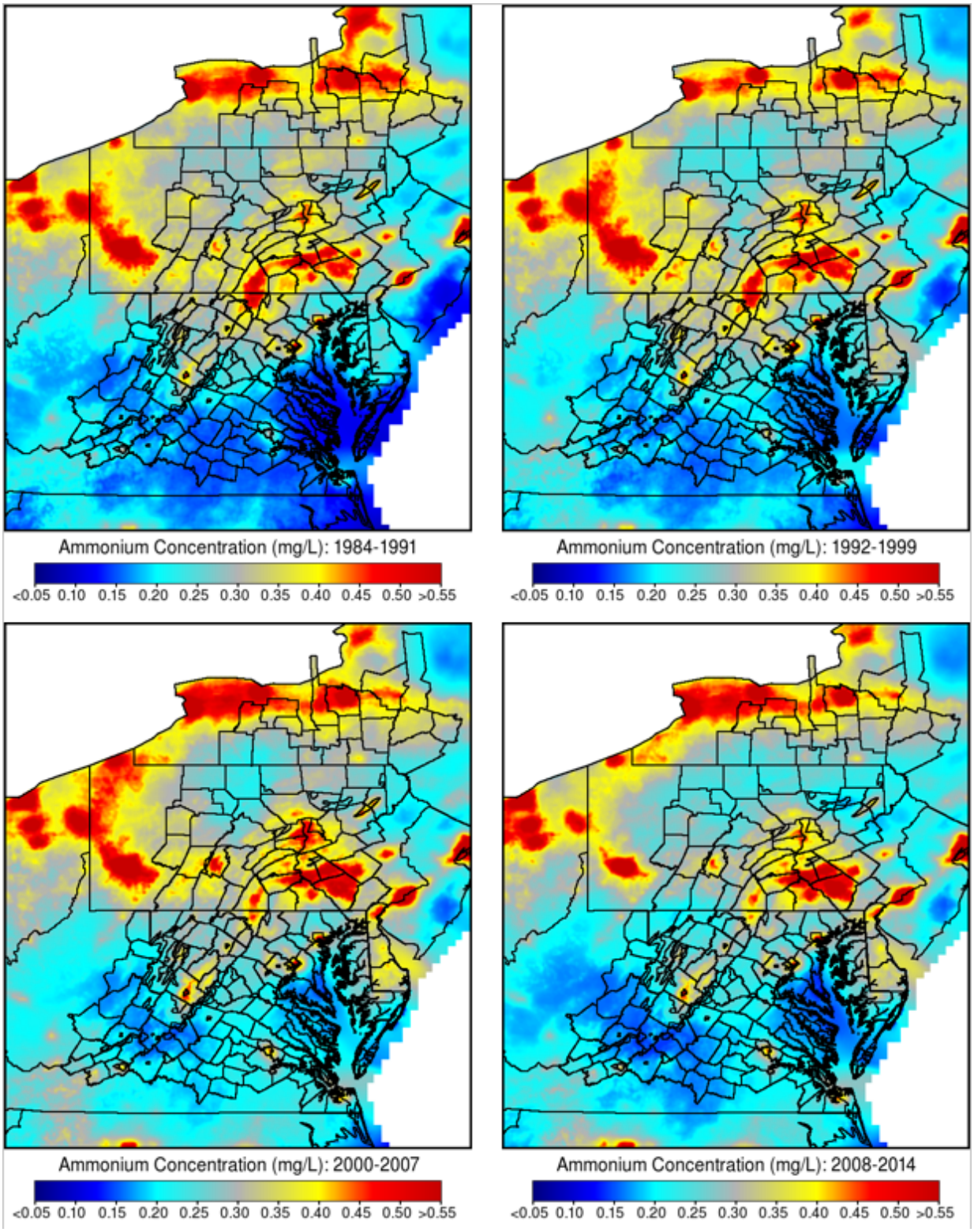

Figure 15. Mean annual ammonium (NH_4) wet-fall concentrations across the Chesapeake Bay Watershed region during four, multi-year summary periods as estimated by the Phase 6 daily ammonium wet-fall concentration model.

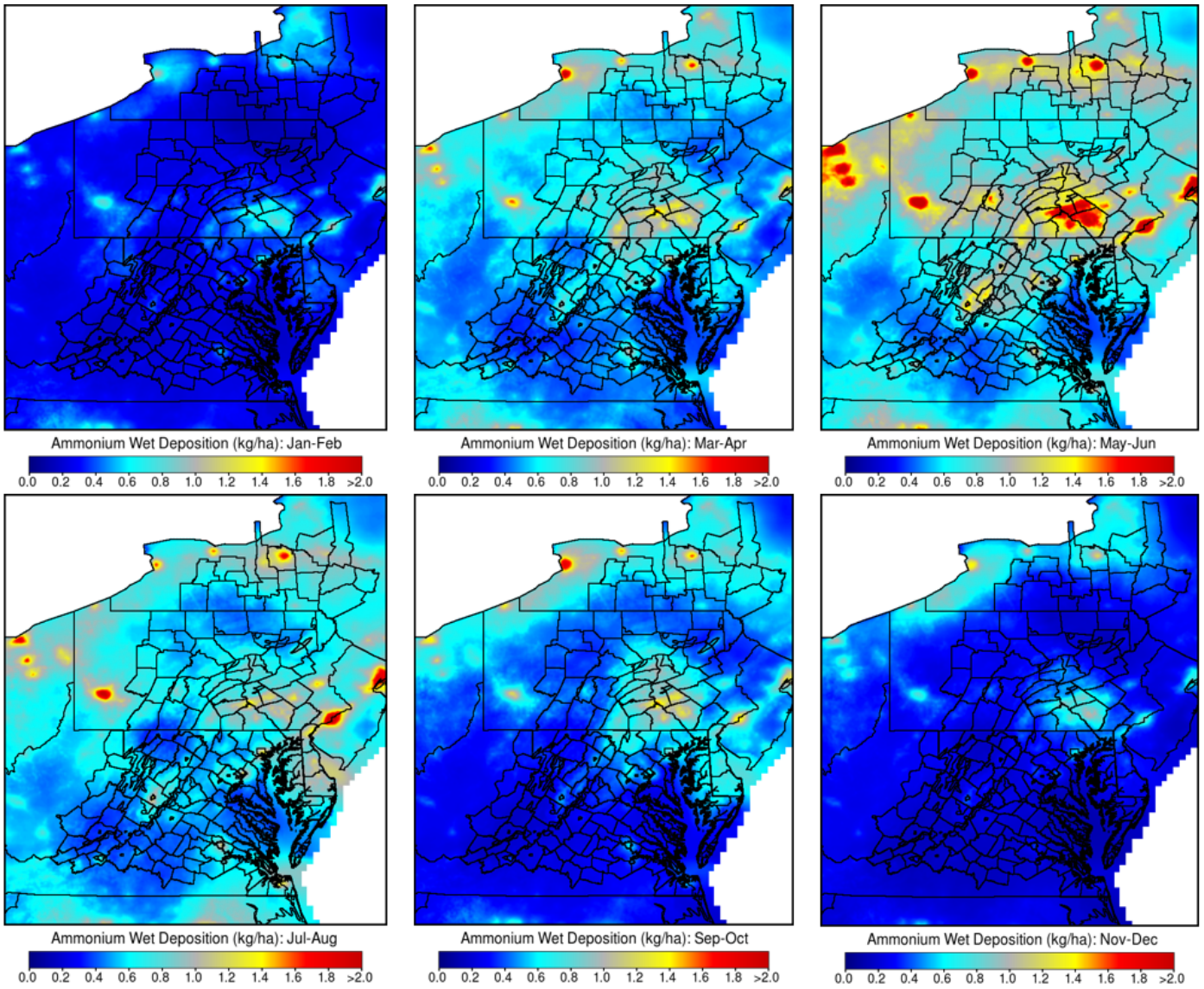

Figure 16. Seasonal mean ammonium (NH_4) wet deposition across the Chesapeake Bay Watershed region during 2010-2014 as calculated by combining Phase 2 daily ammonium wet-fall concentration estimates with precipitation volumes from the NLDAS-2 model.

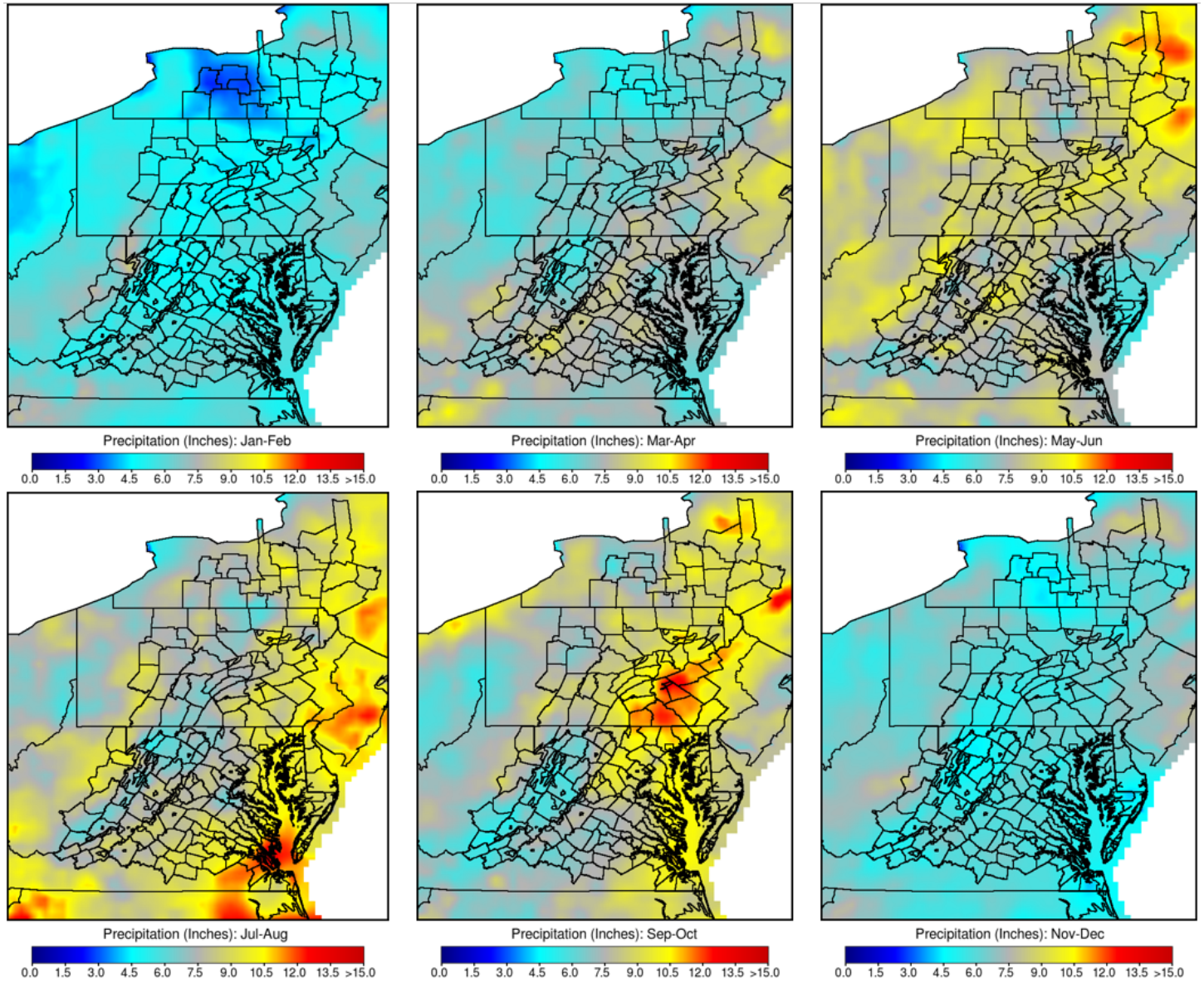

Figure 17. Seasonal mean estimated precipitation from the NLDAS-2 model across the Chesapeake Bay Watershed region during 2010-2014.

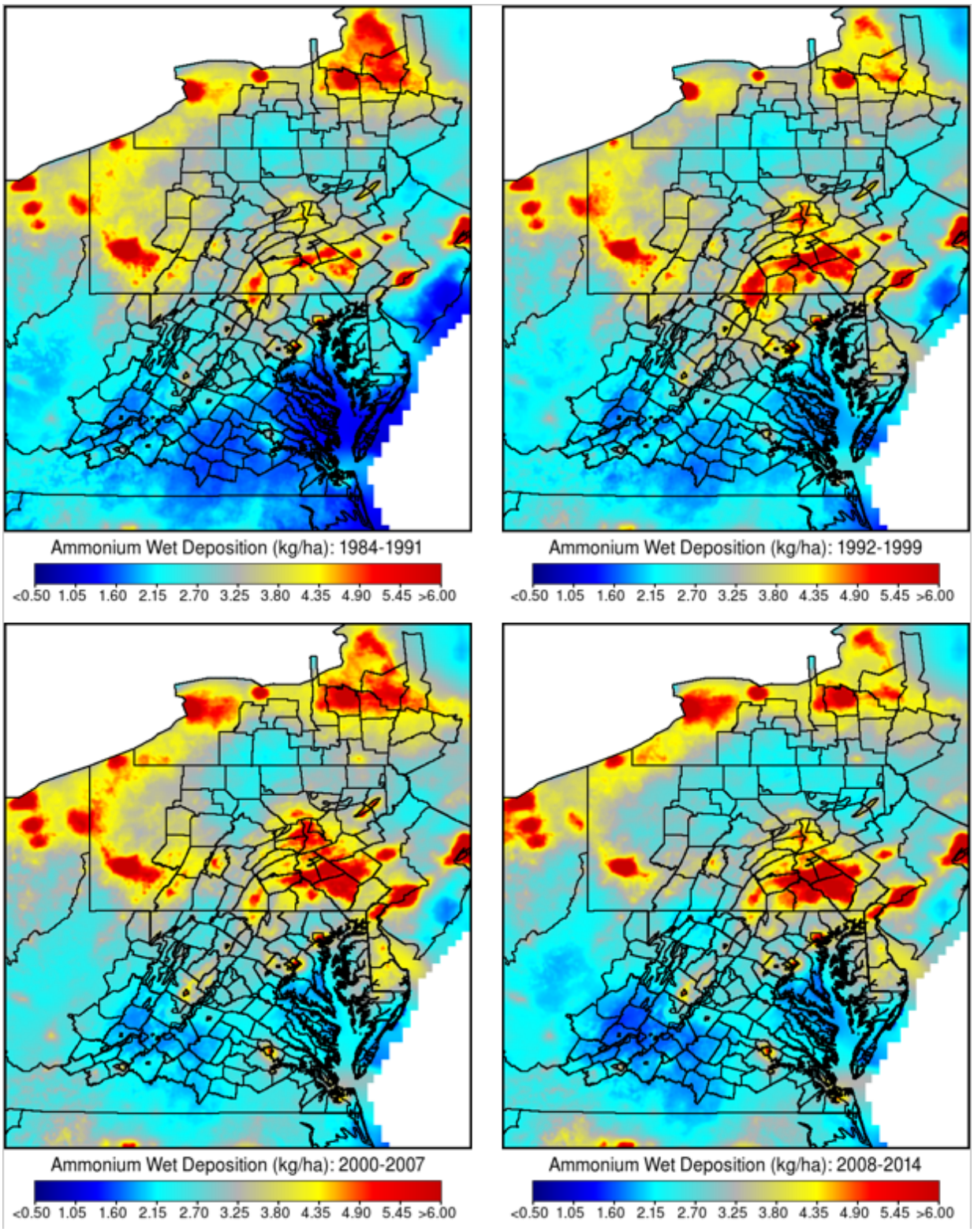

Figure 18. Mean annual ammonium (NH_4) wet deposition across the Chesapeake Bay Watershed region during four, multi-year summary periods as calculated by combining Phase 6 daily ammonium wet-fall concentration estimates with precipitation volumes from the NLDAS-2 model.

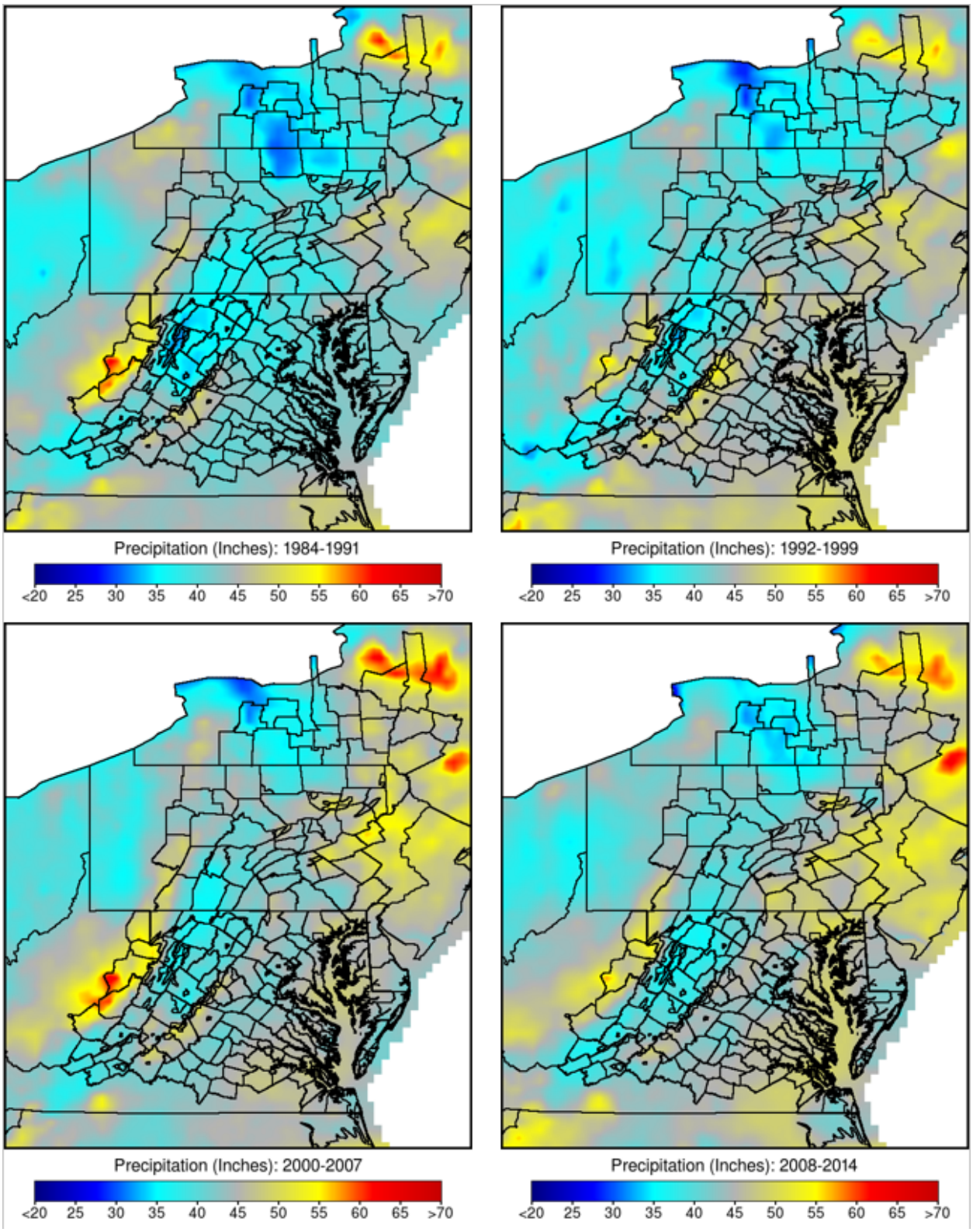

Figure 19. Mean annual estimated precipitation from the NLDAS-2 model for four, multi-year summary periods.

Nitrate Wet-Fall Concentration and Wet Deposition

Model Development

The Phase 6 multiple regression model developed to estimate daily wet-fall nitrate concentrations across the CBW region appears in Table 5. The model is dominated by the inverse relationship between event precipitation volume and nitrate concentrations of samples collected at the 85 NADP/NTN stations (Fig. 21). A strong non-linear long-term temporal trend effect in estimated daily nitrate concentrations is apparent in addition to the pronounced direct relationship with transported facility emissions levels encountered during precipitation event trajectories. Because facility emissions are also subject to long-term temporal trends, interpretation of temporal trends in estimated nitrate concentrations requires additional analyses of the model estimates. Significant seasonal variation in wet-fall nitrate concentrations is evident in the Phase 6 model, but is not as pronounced as the effect in the ammonium concentration model. Nearby crop cultivation levels and short range exposure to residential nitrous oxide emissions also directly contributed to estimated nitrate wet-fall concentrations. Increasing 12-hour antecedent precipitation volumes were associated with decreased nitrate concentrations. As was found with the Phase 6 ammonium concentration model, the anthropogenic covariates did not have a significant seasonal dependency.

The overall fit of the nitrate wet-fall concentration model for the period spanning 1984 through 2014 (Fig. 20, r^2=0.4643) is slightly less than obtained for either NADP/NTN samples collected in and around the CBW modeling region during 1984 through 2001 (r^2=0.4940; Grimm and Lynch, 2005) or for the model developed in our Phase 5 analyses for the sample period 1984 through 2005 (r^2=0.4763; Grimm and Lynch, 2007). As with the Phase 6 ammonium concentration model, the sample data for our latest nitrate concentration model includes data from both an extended span of years, as well as, a much larger set of sampling sites 39 vs 85).

Model Verification

Comparison of single event nitrate nitrogen wet deposition reports from the 36 NADP/NTN sites active in the CBW region with complete precipitation chemistry data for 10 or more years during 1984 through 2014 with estimates derived for the Phase 6 nitrate wet-fall concentration model shows that, on average, the Phase 6 model underestimated nitrate nitrogen wet deposition by only 0.27 percent (Table 6). The largest mean bias in estimated of event nitrate nitrogen wet deposition occurred at NY29 (-3.04 percent). Mean absolute errors for event nitrate nitrogen wet deposition estimates ranged from 5.81 percent at NY52 to 7.85 at NC03 and averaged 6.54 percent. The mean correlation between single event nitrate nitrogen wet deposition reports from the 36 long-term NADP/NTN sites and estimates derived from the Phase 6 nitrate model was 0.6751 and was an improvement over the corresponding correlation reported for our earlier nitrate wet-fall concentration model (0.5879; Grimm and Lynch, 2005).

The mean percent absolute difference between annual nitrate nitrogen wet depositions reported by the 36 NADP/NTN sites in the CBW region during 1984 through 2014 and the estimates from the Phase 6 nitrate model (Table 7, 1.79 percent) improves on the 15.5 percent rate obtained from our initial nitrate concentration model (Grimm and Lynch, 2005) and the 4.08 percent mean absolute error from the Phase 5 model (Grimm and Lynch, 2007). The mean bias of annual nitrate wet deposition estimates at the 36 long-term NADP/NTN sites for the Phase 6 model is 0.28 percent. The mean temporal correlation between annual wet deposition estimates from the Phase 6 nitrate model and annual nitrate wet deposition observations from the 36 long-term NADP/NTN stations was 0.9522. As with the Phase 6 ammonium model, the agreement between reported annual nitrate depositions and the Phase 6 estimates is sufficient to describe spatial patterns and long-term trends in nitrate wet deposition throughout the CBW modeling domain during 1984 through 2014.

Table 5. Linear least-squares model of daily nitrate (NO_3^-) wet-fall concentration for the Chesapeake Bay modeling region for developed from measures of long-term trend, seasonality, spatial location, precipitation volume, precipitation event history, land-use composition, and both transported emissions and static spatial distributions of emissions sources. The temporal scope of the model is from 1984 through 2014.

Dependent Variable: log10([NO_3-(mg/L)])
Number of observations: 13,843 Model r^2: 0.4643

Predictor	Coefficient	DF	Type III Sum of Squares	p
intercept	-1.76745			<0.0001
event precipitation (inches)	0.09942	1	8.078	<0.0001
sqrt(event precipitation (inches))	-0.67309	1	77.227	<0.0001
12hr antecedent precipitation (inches)	-0.38667	1	6.296	<0.0001
event date - 1966 (as decimal year)	-0.06932	1	21.214	<0.0001
sqrt(event date - 1966)	0.71896	1	17.411	<0.0001
cool season (1 during September through January, 0 during February through August)	-0.09324	1	4.762	<0.0001
bimonthly season of event (6 categorical levels)		5	14.395	<0.0001
jan-feb	0.04122			
mar-apr	0.07892			
may-jun	0.12288			
jul-aug	0.16250			
sep-oct	0.02401			
nov-dec	0.00000			

Table 5 (continued).

Predictor	Coefficient	DF	Type III Sum of Squares	p
log10(mean concentration of transported facility emissions during 24-hour back-trajectory)	0.12046	1	40.469	<0.0001
sqrt(mean concentration of transported facility emissions during 6-hour back-trajectory (weighted by atmospheric precipitable water))	0.00185	1	3.827	<0.0001
sqrt(cropland use with 10km (inverse distance-weighted relative fraction))	0.10156	1	6.354	<0.0001
log10(mean concentration of transported residential emissions during 6-hour back-trajectory)	0.04417	1	4.166	<0.0001

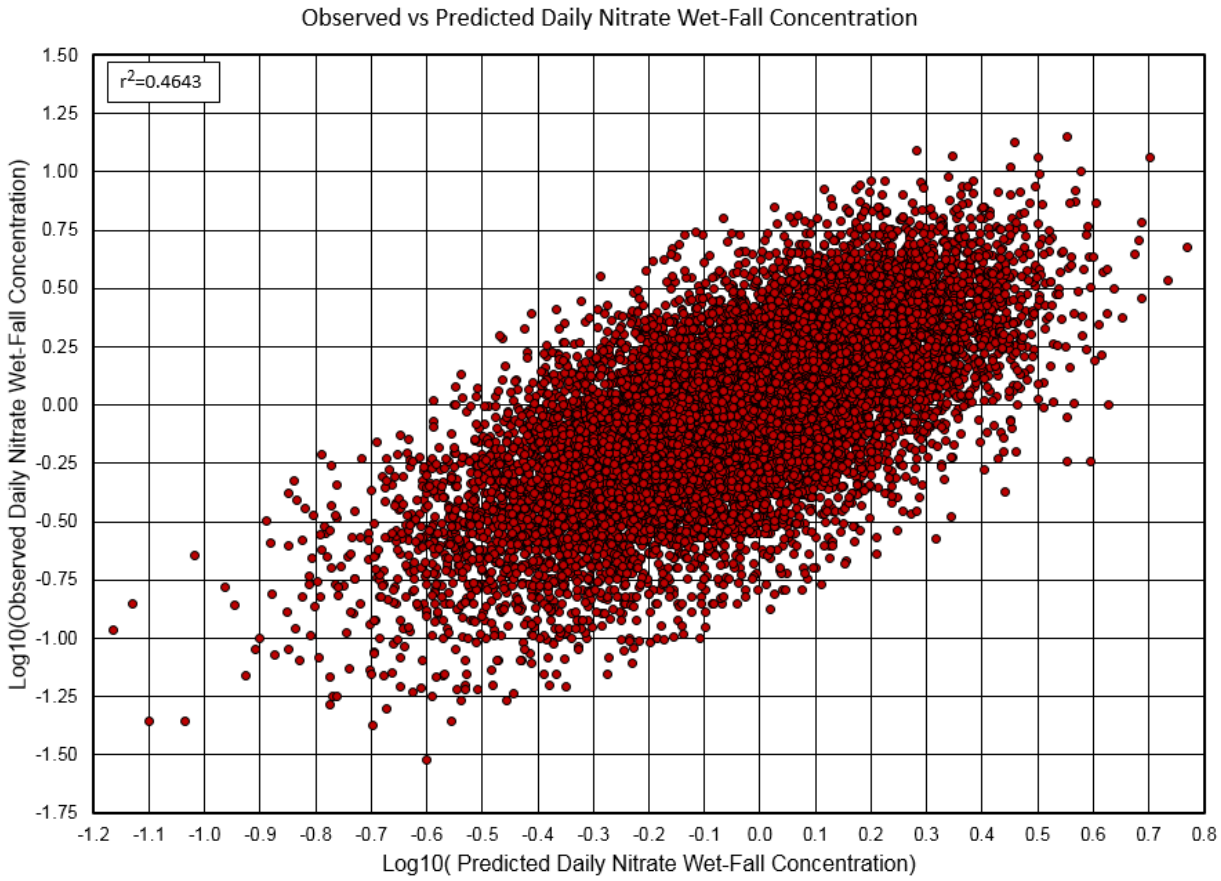

Figure 20. Comparison of estimates from the Phase 6 daily nitrate (NO_3^-) wet-fall concentration model to reported measurements of nitrate concentration in single event precipitation samples collected at 85 NADP/NTN and PADM sites in the Chesapeake Bay Watershed modeling domain region during 1984-2014.

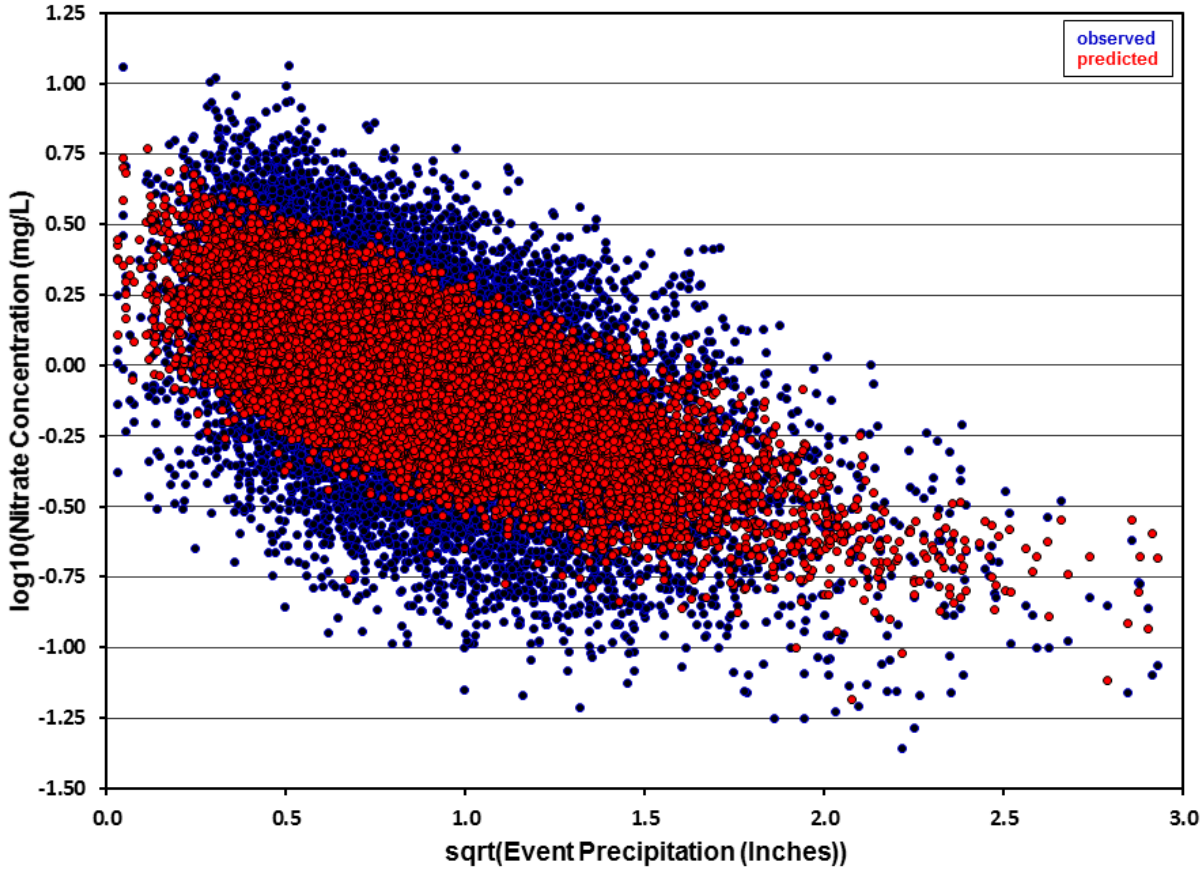

Figure 21. Relationship of observed single-event nitrate (NO_3^-) wet-fall concentrations at 85 NADP/NTN sites in the Chesapeake Bay Watershed region during 1984-2014 and estimates from the Phase 6 daily nitrate wet-fall concentration models to precipitation event volume.

Table 6. Comparison of single event nitrate nitrogen (NH_4-N) wet depositions recorded at long-term 36 NADP/NTN sites located within or adjacent to the CBW region with estimates derived from the Phase 6 nitrate wet-fall concentration model and NLDAS-2 precipitation volumes. Observations for the NADP/NTN sites spanned 1984 through 2014.

Site	Number of Events	Mean Percent Error	Mean Absolute Percent Error	Correlation
ky22	244	-0.32	6.30	0.6762
md03	139	0.12	6.46	0.7095
md08	63	-0.19	6.46	0.6933
md13	255	-0.39	6.73	0.6190
nc03	264	0.20	7.85	0.5552
nc34	243	-0.14	6.51	0.6384
nc41	284	0.44	6.62	0.5798
nj99	317	0.17	7.76	0.5364
ny08	136	0.32	6.59	0.7067
ny10	122	-1.06	6.12	0.7505
ny20	135	-0.80	7.08	0.5855
ny22	69	-0.46	6.20	0.6593
ny29	55	-3.04	5.97	0.7924
ny52	100	0.28	5.81	0.7453
ny65	101	-0.04	6.37	0.7721
ny68	253	-0.23	6.69	0.6027
ny98	114	0.51	6.95	0.7244
ny99	307	-0.93	6.66	0.6484
oh49	206	0.54	6.28	0.6823
oh71	209	0.46	6.14	0.6986
pa00	170	-0.48	6.45	0.6314
pa15	269	-0.28	6.17	0.6606
pa18	149	-0.33	6.23	0.6359
pa29	160	0.07	6.43	0.7036
pa42	247	0.13	6.24	0.6308
pa72	262	-0.74	7.27	0.5918
tn00	236	-0.40	6.20	0.7001
tn04	142	-0.38	6.45	0.7967
tn11	216	0.67	6.55	0.6218
va00	246	-0.60	6.89	0.6084
va13	192	-0.40	6.78	0.6742
va24	153	-0.33	6.76	0.7491
va28	264	-0.27	6.52	0.7250
wv04	134	-0.45	6.67	0.6845
wv05	92	-0.52	5.91	0.7866
wv18	158	-0.76	6.54	0.7280
Mean		-0.27	6.54	0.6751

Table 7. Comparison of annual nitrate nitrogen (NH_4-N) wet depositions recorded at long-term 36 NADP/NTN sites located within or adjacent to the CBW region with estimates derived from the Phase 6 nitrate wet-fall concentration model and NLDAS-2 precipitation volumes. Observations for the NADP/NTN sites spanned 1984 through 2014.

Site	Number of Years	Mean Observed Deposition ------ kg N/ha --------	Mean Estimated Deposition	Mean Percent Error	Mean Absolute Percent Error	Temporal Correl.
KY22	31	2.6224	2.6142	-0.22	1.54	0.9682
MD03	16	3.6871	3.6772	-0.17	1.28	0.9238
MD08	10	1.7943	1.8385	2.71	2.96	0.9212
MD13	30	2.7677	2.7744	0.26	1.44	0.9640
NC03	31	2.0879	2.1067	0.95	1.57	0.9771
NC34	30	2.3157	2.3364	0.87	1.97	0.9529
NC41	28	2.1027	2.1075	0.24	0.94	0.9647
NJ99	30	3.2410	3.3110	1.96	3.71	0.9065
NY08	31	3.0917	3.1292	1.26	1.56	0.9509
NY10	18	4.4622	4.4635	0.07	1.87	0.9615
NY20	30	2.7904	2.7872	-0.12	1.41	0.9796
NY22	12	2.5312	2.5251	-0.22	1.16	0.9241
NY29	11	2.4569	2.4514	-0.26	1.11	0.9442
NY52	23	5.7466	5.8059	1.23	3.18	0.9071
NY65	17	2.7550	2.7866	1.14	1.39	0.9370
NY68	28	3.7168	3.6978	-0.50	1.98	0.9616
NY98	27	2.6151	2.5932	-0.71	1.74	0.9787
NY99	28	3.8600	3.8918	0.82	2.37	0.9114
OH49	30	3.5538	3.5582	0.17	1.01	0.9876
OH71	31	3.1121	3.1128	0.01	1.12	0.9330
PA00	15	2.8388	2.8432	0.33	2.04	0.9292
PA15	30	3.5466	3.5778	0.87	2.39	0.9308
PA18	14	2.8416	2.8572	0.51	1.49	0.9785
PA29	48	4.0199	4.0310	0.40	1.34	0.9616
PA42	30	3.8256	3.8402	0.42	1.38	0.9333
PA72	24	3.6271	3.6514	0.69	2.61	0.9407
TN00	25	2.9268	2.9186	-0.19	0.85	0.9893
TN04	15	2.1819	2.1627	-0.74	1.40	0.9775
TN11	29	2.7182	2.7125	-0.17	1.84	0.9698
VA00	24	2.8809	2.8093	-2.28	2.88	0.9057
VA13	23	2.1202	2.1257	0.28	1.37	0.9306
VA24	15	1.9776	1.9446	-0.56	3.10	0.8903
VA28	21	2.2625	2.2727	0.28	1.49	0.9693
WV04	19	3.3563	3.3627	0.23	1.59	0.9492
WV05	14	2.5384	2.5721	1.06	1.85	0.9776
WV18	30	3.6902	3.6595	-0.69	1.41	0.9418
Mean		3.0184	3.0253	0.28	1.79	0.9481

Spatial Patterns and Temporal Trends in Nitrate Wet-Fall Concentration and Wet Deposition

In comparison to the Phase 6 ammonium wet-fall concentration estimates, the distribution of Phase 6 nitrate wet-fall concentrations across the CBW regions show a more consistent spatial pattern among seasons (Fig. 22). Estimated nitrate concentrations are consistently highest over the Susquehanna River Basin in central Pennsylvania and the northern periphery of the CBW modeling domain in New York. Peak nitrate concentrations occur in areas where the influx of nitrous oxide emissions from facility and residential sources coincide with intensive crop production, such as to the south and east of Buffalo, Rochester, and Syracuse, New York and across central and eastern Pennsylvania where seasonal air flow and storm tracks carry nitrous oxide emissions from the numerous facility sources located to the west and within the region over areas of abundant cropland and livestock production (See Figs. 3 and 4). Throughout most of the CBW modeling domain, nitrate wet-fall concentrations are generally highest in winter and early spring and reach a minimum in September and October. The influence of nitrous oxide emissions from facility sources in the Phase 6 nitrate wet-fall concentration model is consistently evident in the mean annual nitrate concentration maps (Fig. 23) for the four summary periods spanning the 1984 through 2014. Progressively declining nitrate concentration estimates throughout the 1984 through 2014 modeling period is also apparent in Figure 23.

Unlike ammonium wet deposition, spatial patterns in estimated seasonal nitrate wet deposition (Fig. 24) are strongly influenced both precipitation volumes (Fig. 17) and nitrate concentration patterns (Fig. 22). The joint influence of both precipitation and concentration patterns on seasonal nitrate wet deposition, but not ammonium wet deposition, may indicate that atmospheric precursors of nitrate are removed by precipitation at a lower rate than are precursors for ammonium. Peak estimate nitrate wet deposition occurs from May through August when both precipitation volumes and nitrate wet-fall concentrations are relatively high. As was noted for estimated annual nitrate concentrations, estimated annual wet deposition rates show a steady decline across nearly all of the CBW from the beginning to end of the 31-year modeling period (Fig. 25).

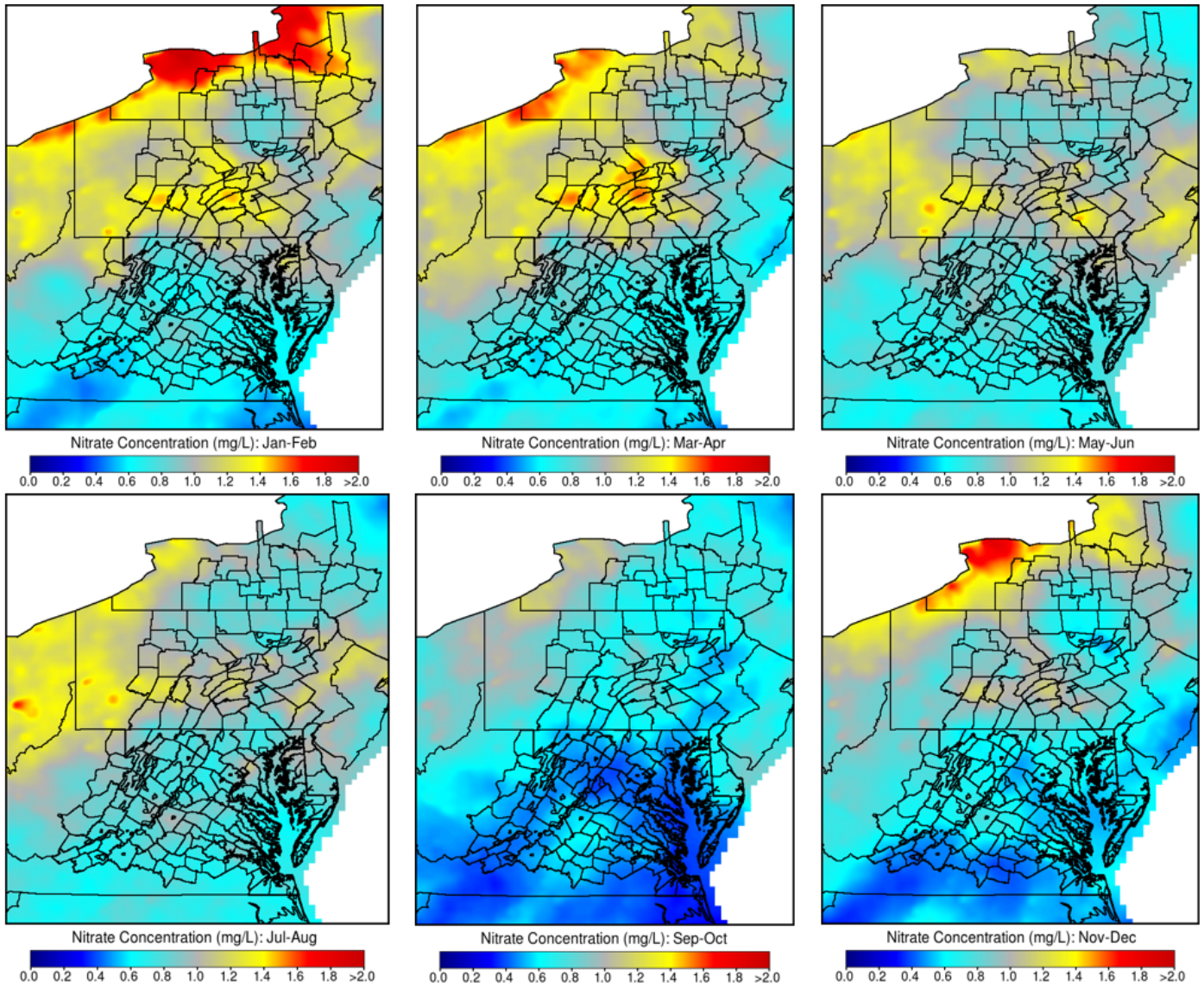

Figure 22. Seasonal mean nitrate (NO_3) wet-fall concentrations across the Chesapeake Bay Watershed region during 2010-2014 as estimated by the Phase 6 daily nitrate wet-fall concentration model.

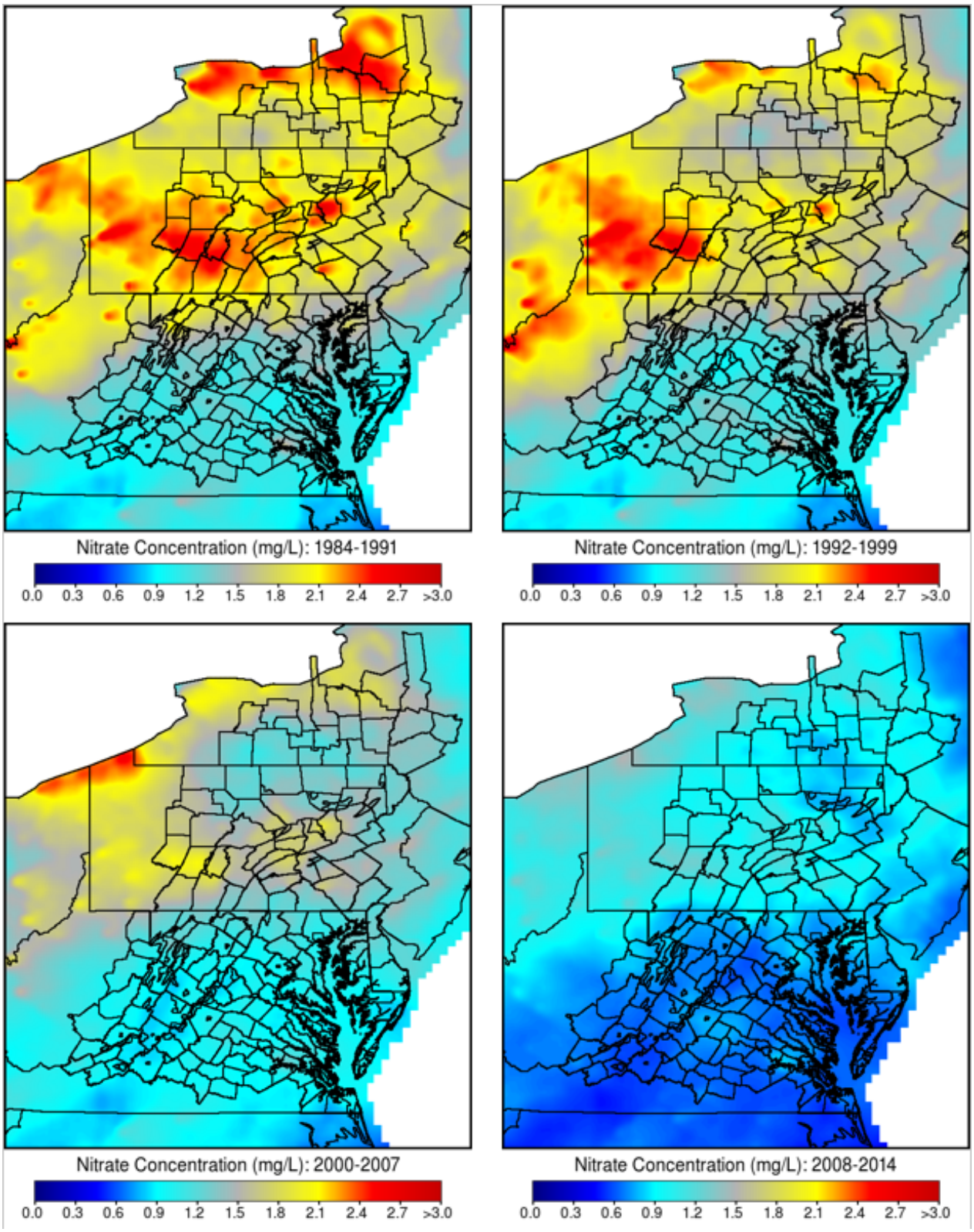

Figure 23. Mean annual nitrate (NO_3) wet-fall concentrations across the Chesapeake Bay Watershed region during four, multi-year summary periods as estimated by the Phase 6 daily nitrate wet-fall concentration model.

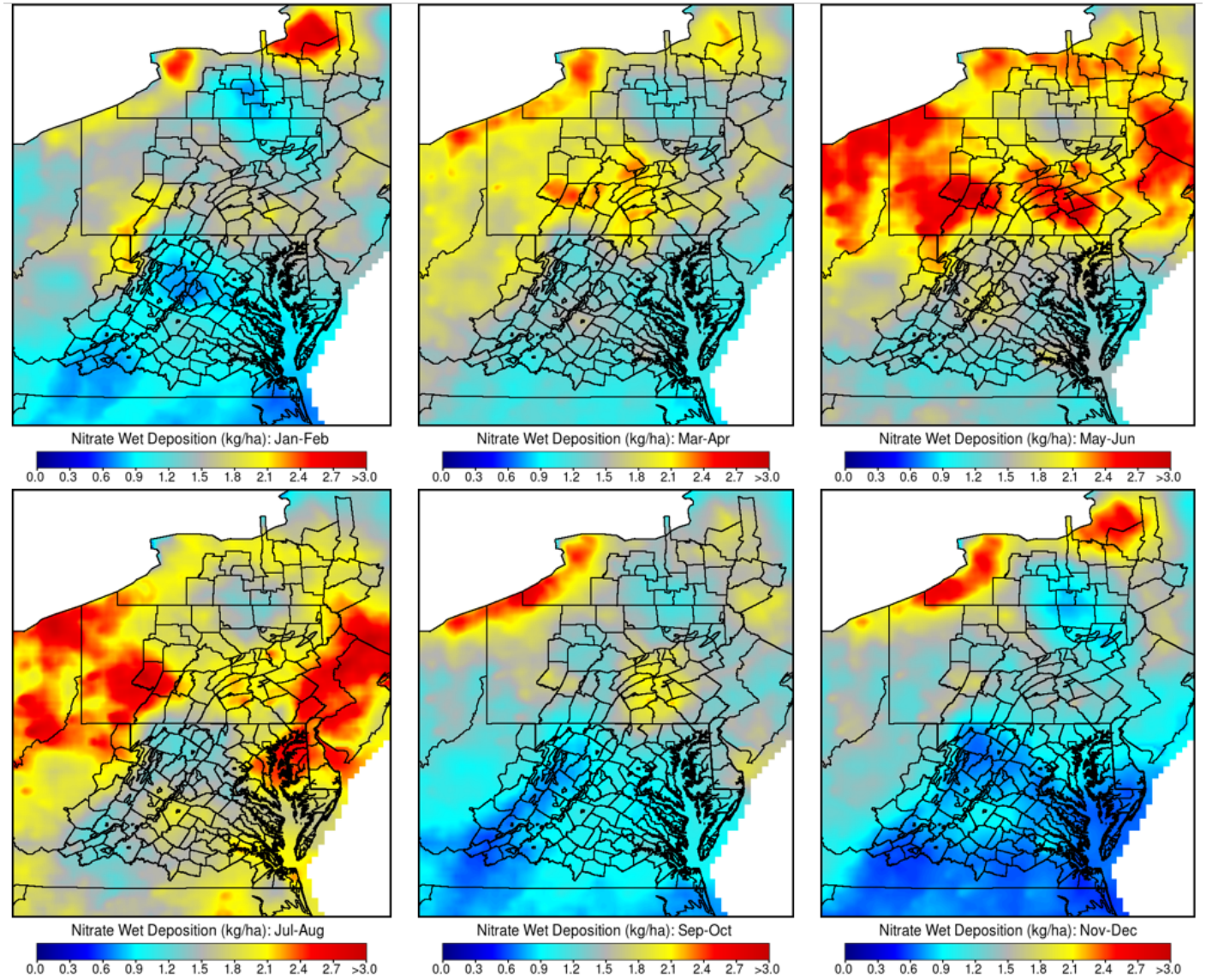

Figure 24. Seasonal mean nitrate (NO_3) wet deposition across the Chesapeake Bay Watershed region during 2010-2014 as calculated by combining Phase 6 daily nitrate wet-fall concentration estimates with precipitation volumes from the NLDAS-2 model.

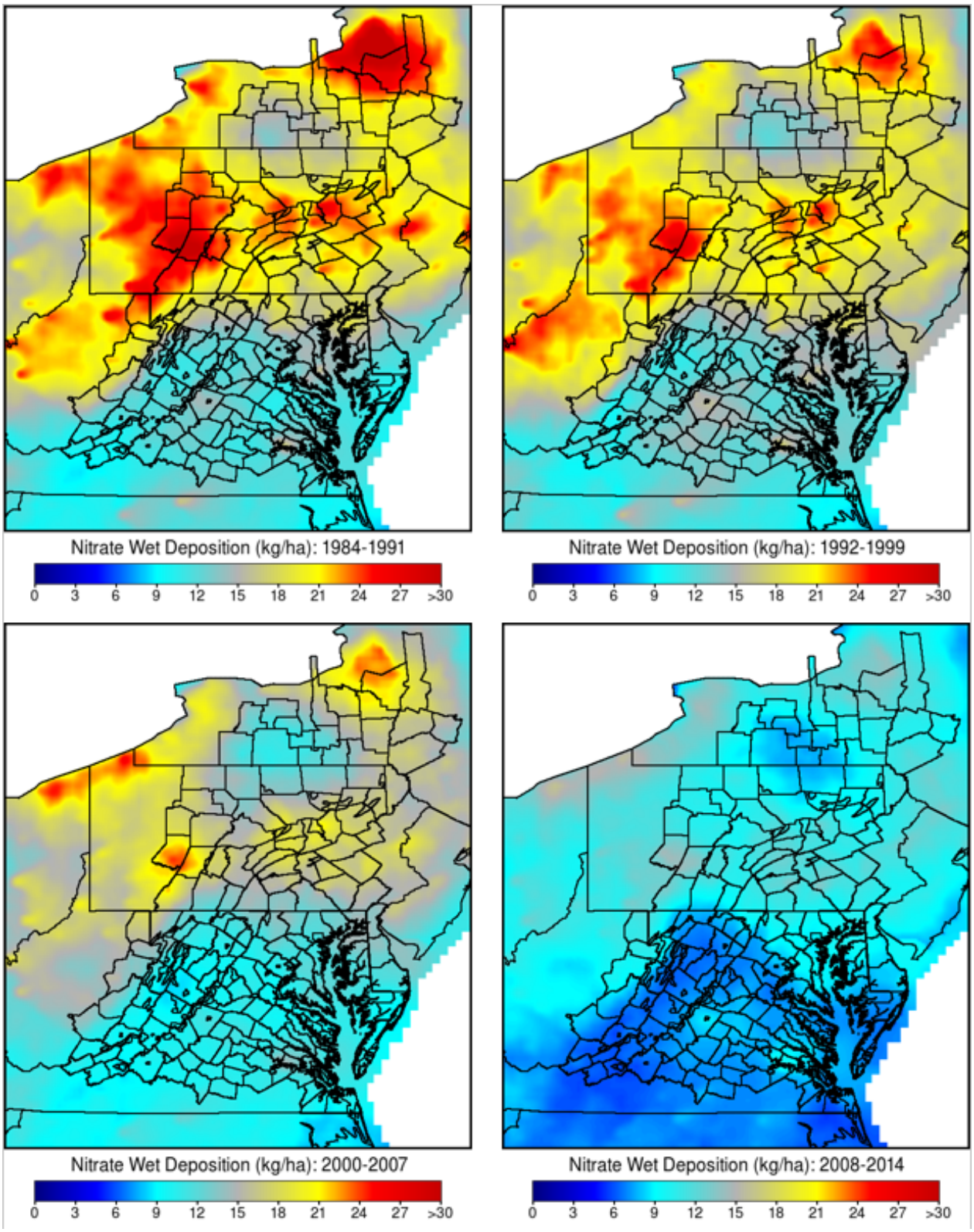

Figure 25. Mean annual nitrate (NO_3) wet deposition across the Chesapeake Bay Watershed region during four, multi-year summary periods as calculated by combining Phase 6 daily nitrate wet-fall concentration estimates with precipitation volumes from the NLDAS-2 model.

Total Inorganic Nitrogen Wet-Fall Concentration and Wet Deposition

Model Verification

Inorganic nitrogen compounds found in precipitation across the eastern U. S. are comprised almost entirely for ammonium and nitrate. Although the models developed in this study estimate ammonium and nitrate concentrations separately, estimates of total inorganic nitrogen wet-fall (TIN) concentration and wet deposition can be reasonably obtained by the summation of the ammonium nitrogen (NH_4-N) and nitrate nitrogen (NO_3-N) concentration and deposition estimates produced by the two species-specific concentration models.

The Phase 6 models jointly over-estimated annual TIN wet depositions reported at the 36 long-term NADP/NTN sites in and around the CBW region during 1984 through 2014 by an average of 0.33 percent (Table 8) and the mean absolute percent error was 1.96 percent. The mean temporal correlation between annual TIN wet deposition estimates from the Phase 6 nitrate model and wet deposition observations from the 36 long-term NADP/NTN stations was 0.9350.

Spatial Patterns and Temporal Trends in Total Inorganic Nitrogen Wet-Fall Concentration and Wet Deposition

As can be expected, the seasonal spatial patterns of TIN wet-fall concentration (Fig. 26) and wet deposition (Fig. 28) across the CBW region, as estimated by combination of the two Phase 6 models, show similarities to the seasonal spatial patterns of both ammonium and nitrate and the major anthropogenic factors influencing the two nitrogen species. The ammonium nitrogen component reflects the spatial distribution of livestock and crop production activities and residential development. The nitrate nitrogen component is heavily influenced by the distribution of facility nitrous oxides emissions. Estimated TIN concentrations are markedly higher from March through August, concurrent with seasonal crop production activities and elevated soil temperature, and then abruptly drop to minimum levels during September and October when precipitation volumes are relatively high and the crop production season completes. Estimated TIN concentrations rebound slightly from November through February as seasonal precipitation volumes fall to their lowest levels. The Phase 6 models indicate that TIN concentrations are highest across the northern half of the CBW region throughout the year. Figures 27 and 29 indicate a widespread decline in annual TIN wet-fall concentration and deposition estimates over the 1984 through 2014 modeling period. The broadly declining trend in estimated TIN wet-fall concentrations and depositions reflect the widespread decline in nitrate nitrogen component, which more than offset any localized increases in the ammonium nitrogen component.

Table 8. Comparison of annual total inorganic nitrogen (NH_4-N + NO_3-N) wet depositions recorded at 36 long-term NADP/NTN sites located within or adjacent to the CBW region with estimates derived from the Phase 6 ammonium and nitrate wet-fall concentration models and NLDAS-2 precipitation volumes. Observations for the NADP/NTN sites spanned 1984 through 2014.

Site	Number of Years	Mean Observed Deposition ------ kg N/ha --------	Mean Estimated Deposition	Mean Percent Error	Mean Absolute Percent Error	Temporal Correl.
KY22	31	4.2750	4.2687	-0.01	1.65	0.9410
MD03	16	5.7380	5.7295	-0.05	1.51	0.9836
MD08	10	3.2890	3.3888	3.34	3.34	0.9042
MD13	30	4.7379	4.7357	-0.01	1.27	0.9675
NC03	31	3.9722	4.0024	0.84	1.58	0.9543
NC34	30	4.7854	4.8474	1.46	2.43	0.9081
NC41	28	4.8498	4.8770	0.58	1.03	0.9029
NJ99	30	5.3510	5.4574	1.90	3.95	0.8978
NY08	31	5.7749	5.8136	0.70	1.43	0.9225
NY10	18	7.4038	7.4247	0.29	1.65	0.9913
NY20	30	4.4034	4.3780	-0.64	1.61	0.9339
NY22	12	4.7222	4.7139	-0.25	1.21	0.9705
NY29	11	4.5485	4.5637	0.27	1.14	0.9209
NY52	23	9.3698	9.4423	0.91	2.92	0.9745
NY65	17	4.3427	4.3814	0.92	1.42	0.9556
NY68	28	5.8965	5.8605	-0.50	2.37	0.9116
NY98	27	4.4244	4.3925	-0.55	1.84	0.8960
NY99	28	5.9635	6.0457	1.34	2.78	0.9349
OH49	30	5.8859	5.8939	0.18	1.36	0.9281
OH71	31	5.9778	5.9867	0.18	1.08	0.9746
PA00	15	5.9126	5.9392	0.75	2.26	0.9266
PA15	30	5.7039	5.7818	1.49	2.93	0.9050
PA18	14	4.9381	4.9560	0.48	1.91	0.9562
PA29	48	6.5283	6.5119	-0.15	1.93	0.9494
PA42	30	6.0929	6.1336	0.70	1.68	0.9268
PA72	24	5.5503	5.6119	1.01	3.01	0.9007
TN00	25	4.9025	4.9097	0.28	1.09	0.9355
TN04	15	4.2427	4.2080	-0.74	1.32	0.9116
TN11	29	4.7227	4.6790	-0.76	2.14	0.9583
VA00	24	4.8568	4.7731	-1.53	2.96	0.9009
VA13	23	3.6857	3.6887	0.13	1.47	0.9031
VA24	15	3.6104	3.5482	-0.75	3.28	0.9024
VA28	21	4.5044	4.4839	-0.58	1.89	0.9600
WV04	19	5.2310	5.2240	-0.10	1.59	0.9726
WV05	14	4.2478	4.3151	1.31	2.16	0.9447
WV18	30	5.8788	5.8366	-0.59	1.36	0.9329
Mean		5.1756	5.1890	0.33	1.96	0.9350

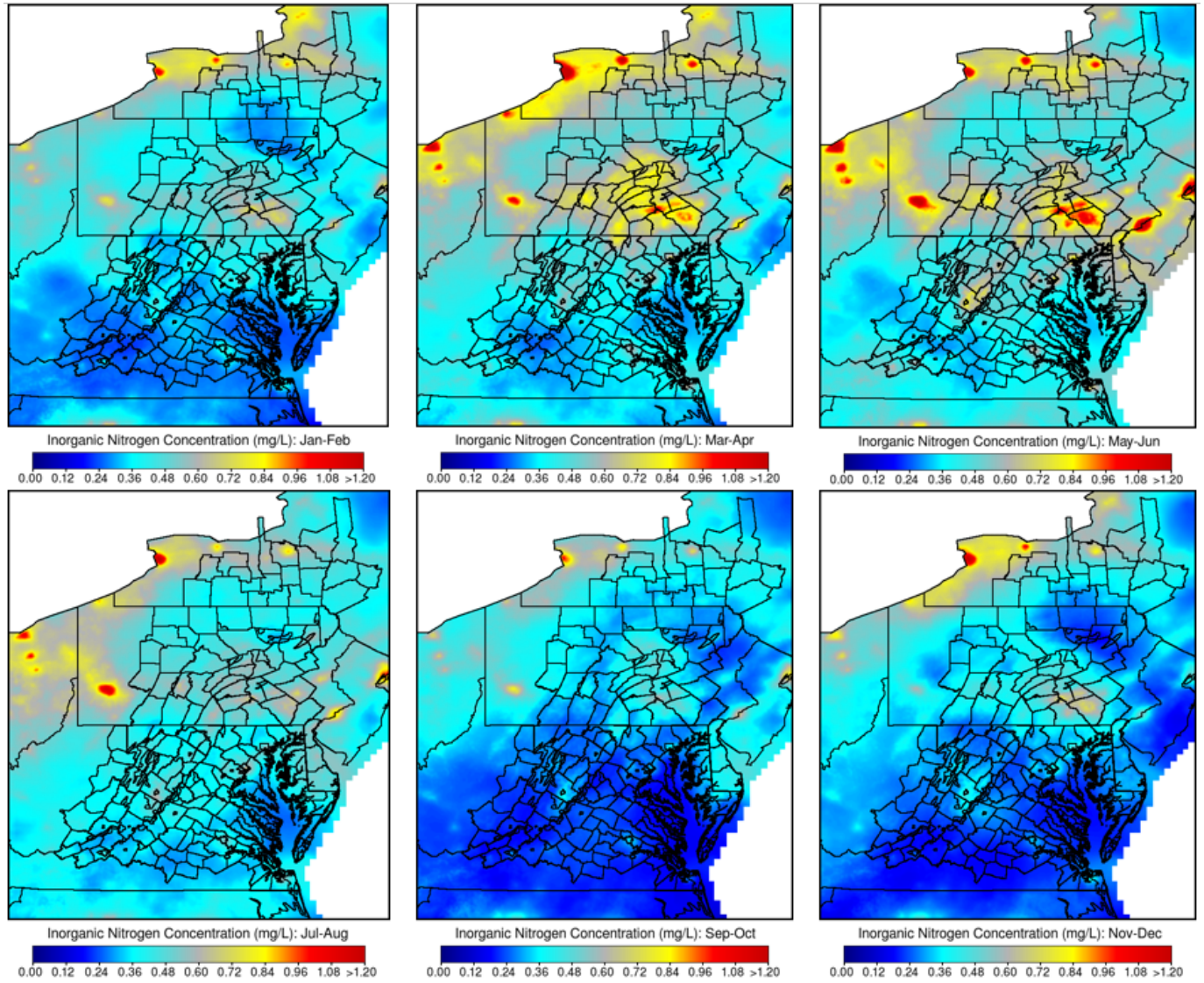

Figure 26. Seasonal mean inorganic nitrogen (NH_4-N + NO_3-N) wet-fall concentrations across the Chesapeake Bay Watershed region during 2010-2014 as estimated by the Phase 6 daily ammonium and nitrate wet-fall concentration models.

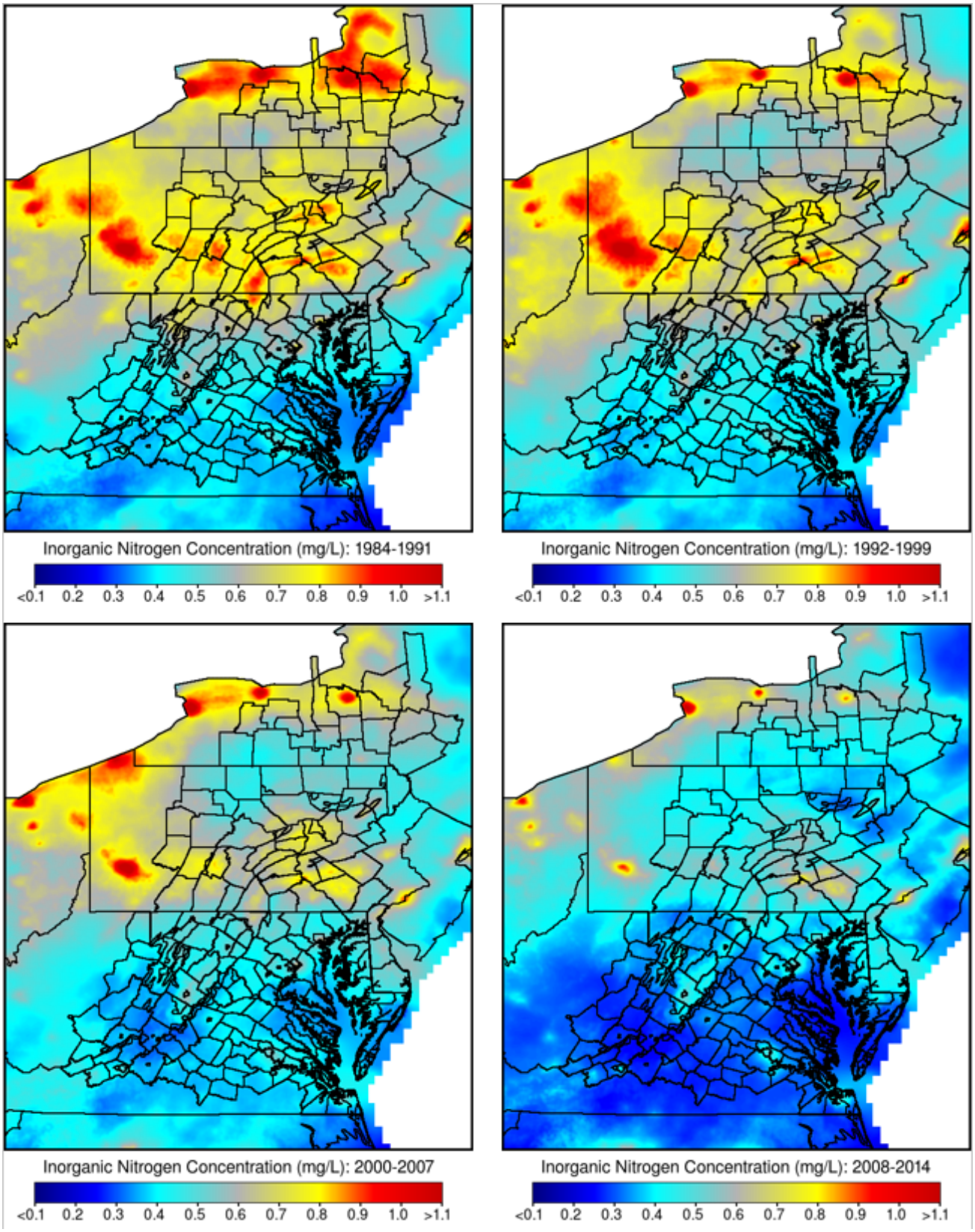

Figure 27. Mean annual inorganic nitrogen (NH_4-N + NO_3-N) wet-fall concentrations across the Chesapeake Bay Watershed region during four, multi-year summary periods as estimated by the Phase 6 daily ammonium and nitrate wet-fall concentration models.

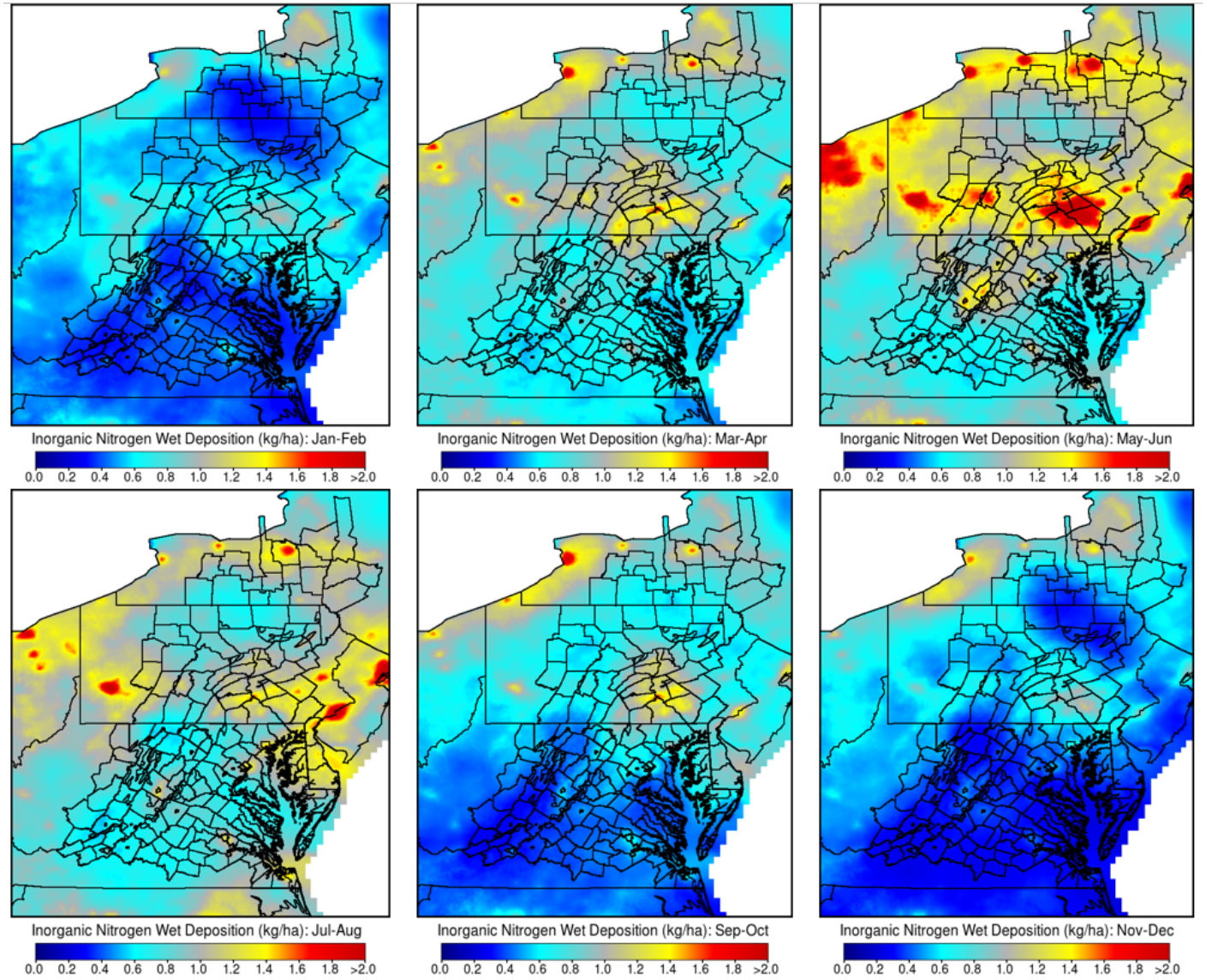

Figure 28. Seasonal mean inorganic nitrogen (NH_4-N + NO_3-N) wet deposition across the Chesapeake Bay Watershed region during 2010-2014 as calculated by combining Phase 6 daily ammonium and nitrate wet-fall concentration estimates with volumes from the NLDAS-2 model.

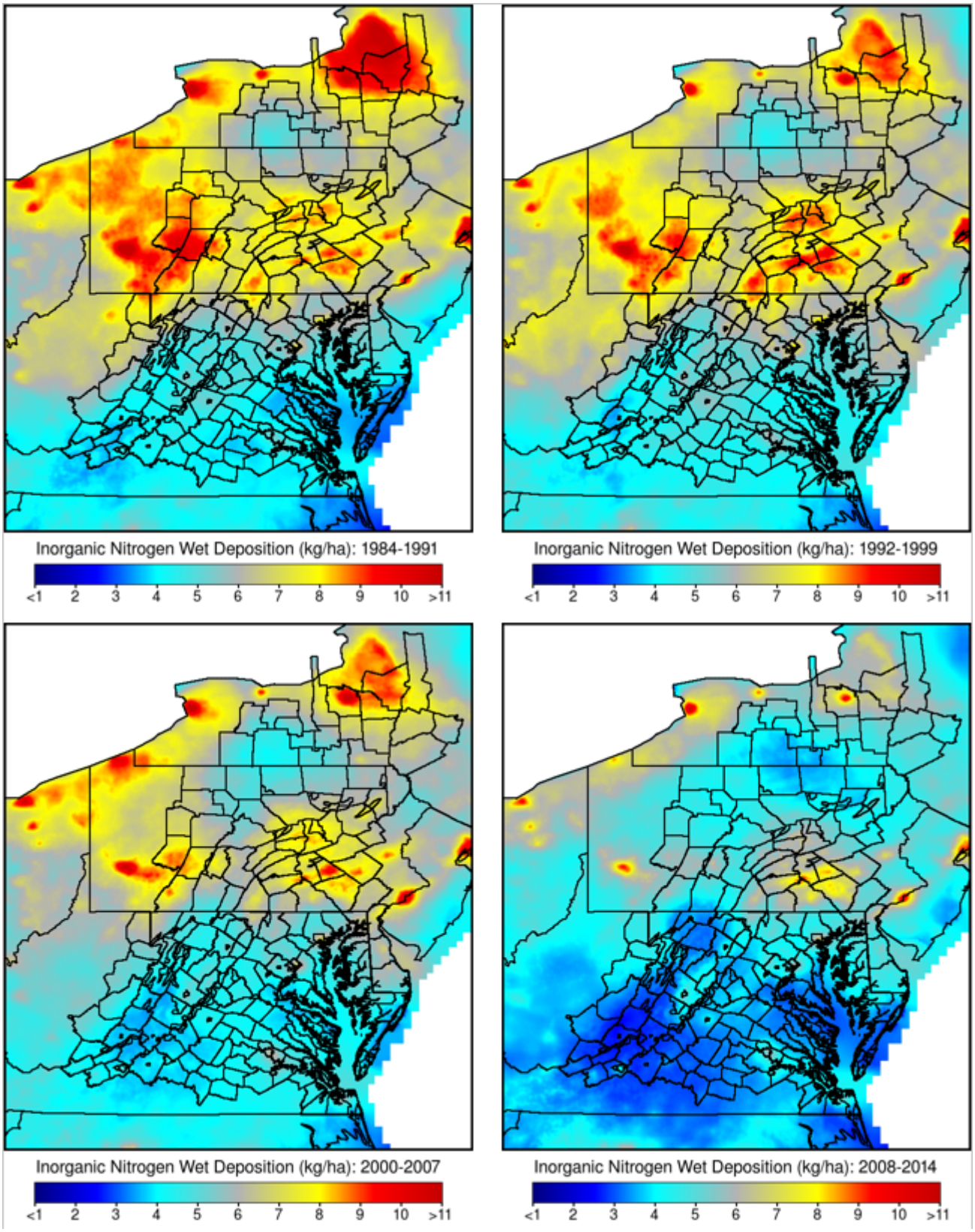

Figure 29. Mean annual inorganic nitrogen (NH_4-N + NO_3-N) wet deposition across the Chesapeake Bay Watershed region during four, multi-year summary periods as calculated by combining Phase 6 daily ammonium and nitrate wet-fall concentration estimates with precipitation volumes from the NLDAS-2 model.

Long-term Trends in Estimated Nitrogen Wet Deposition

Figures 30 through 32 show estimated annual wet deposition rates for nitrate nitrogen, ammonium nitrogen, and TIN for three distinct land segments of the CBW domain throughout the time span of the Phase 6 modeling period and the long-term trend regressions fitted to them. Cortland County, New York is located in the north-central portion of the CBW domain; Adams County, Pennsylvania is the central portion of the domain; and Dorchester County, Maryland is the southern section of the modeling area on the eastern shore of the Chesapeake Bay. All three segments have extensive croplands and limited residential development. Estimated annual nitrate nitrogen depositions declined overall from 1984 through 2014 in all segments, but not in a consistently linear manner; with deposition levels in Dorchester County rising from 1984 through 1993. Estimated annual ammonium nitrogen wet depositions for the two northernmost segments exhibited little overall trend; whereas, in Dorchester County, ammonium nitrogen deposition trended higher from 1984 through 2003 and then began an accelerating decline through the end of the modeling period. Cortland and Adams Counties had estimated annual TIN depositions that declined in a nearly linear pattern from 1984 through 2014. In contrast, the long-term trend function for annual TIN deposition in Dorchester County was markedly non-monotonic. The dissimilarities in nitrogen wet deposition trend profiles demonstrates the need to estimate deposition trends on a small geographic scale with appropriate trend functions, rather than applying a region-wide estimate of deposition tendencies.

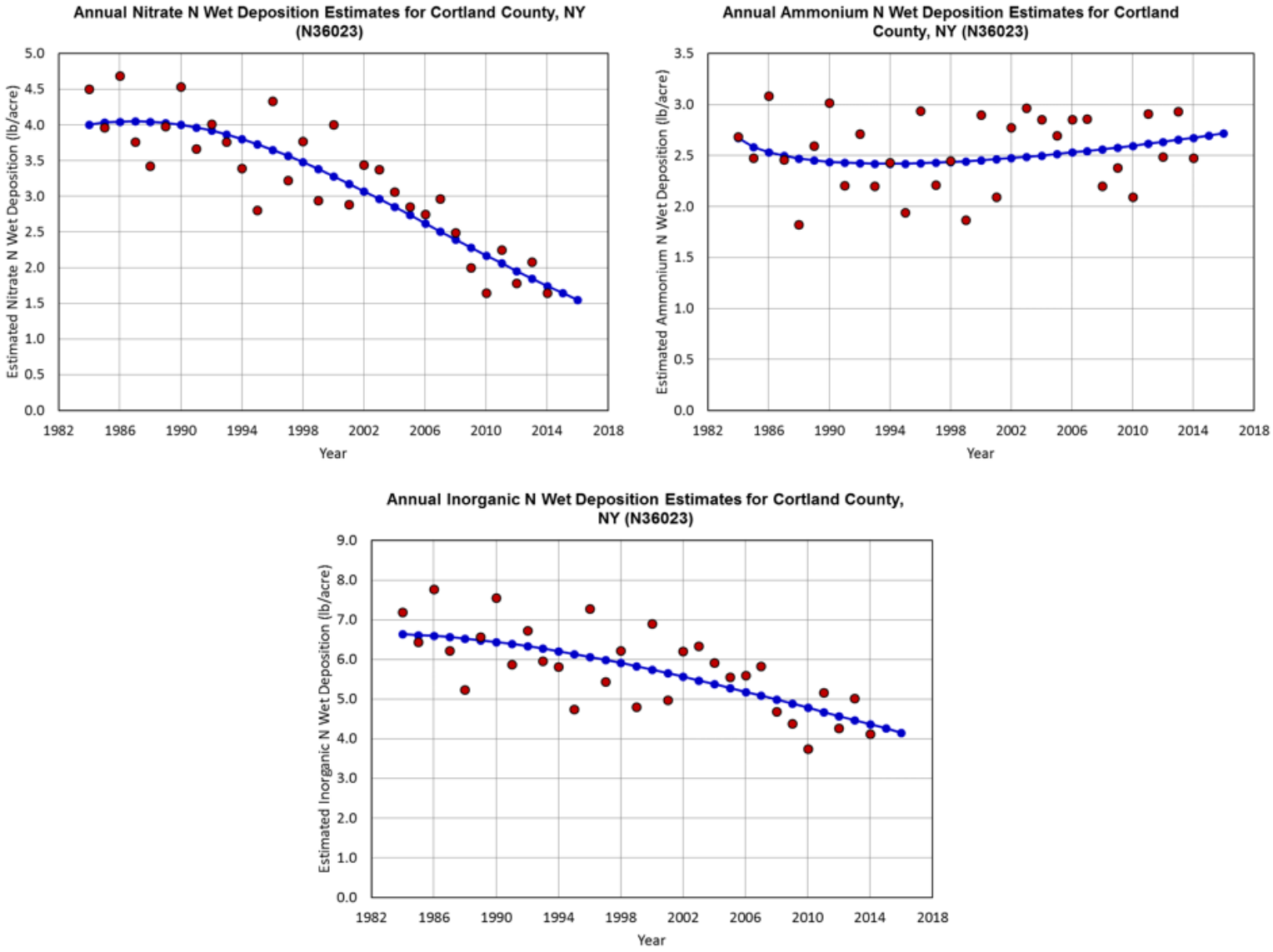

Figure 30. Long-term trends in annual nitrogen wet deposition estimates from the Phase 6 nitrate and ammonium models for Cortland County, New York (Phase 6 land segment N36023).

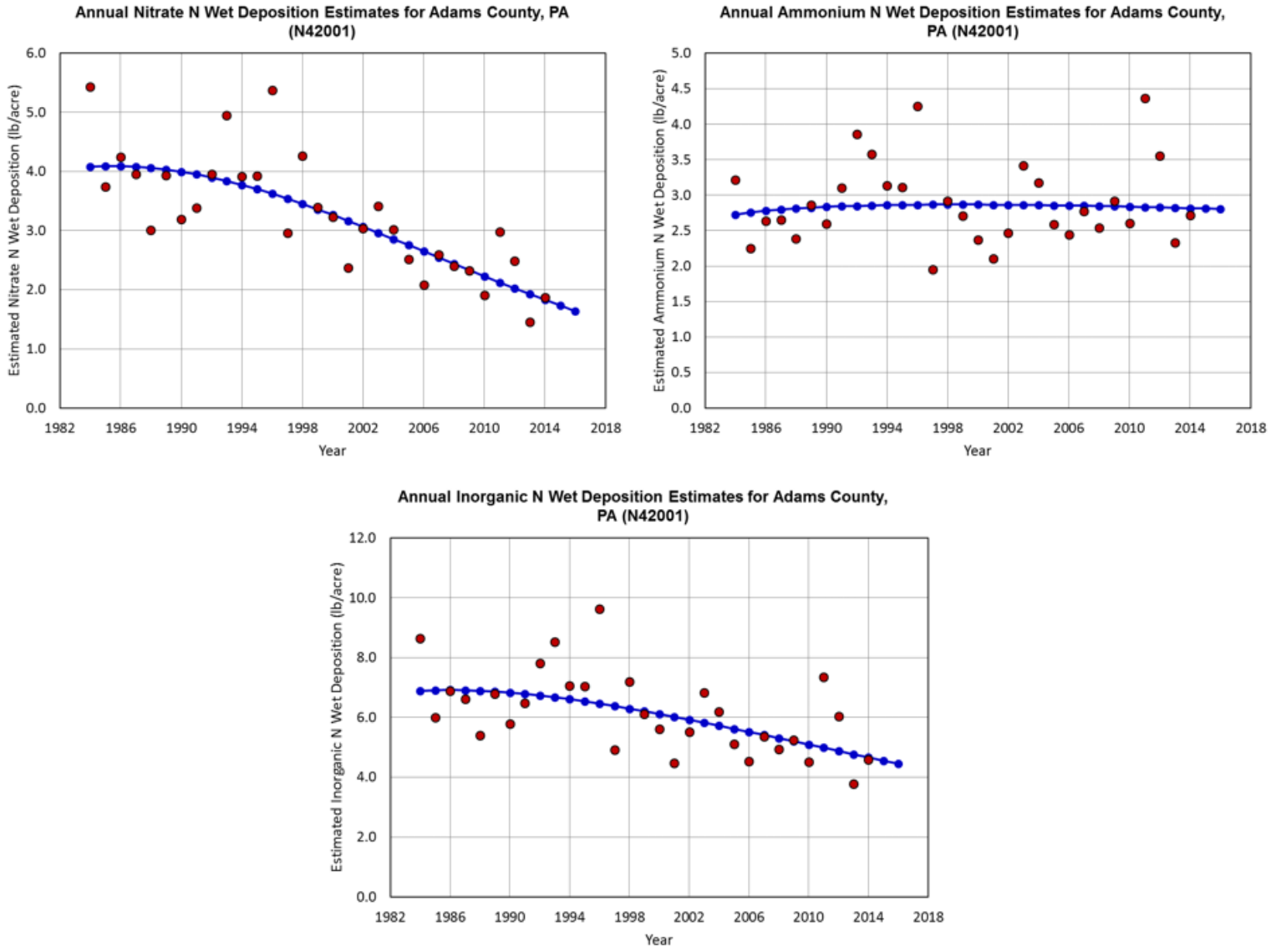

Figure 31. Long-term trends in annual nitrogen wet deposition estimates from the Phase 6 nitrate and ammonium models for Adams County, Pennsylvania (Phase 6 land segment N42001).

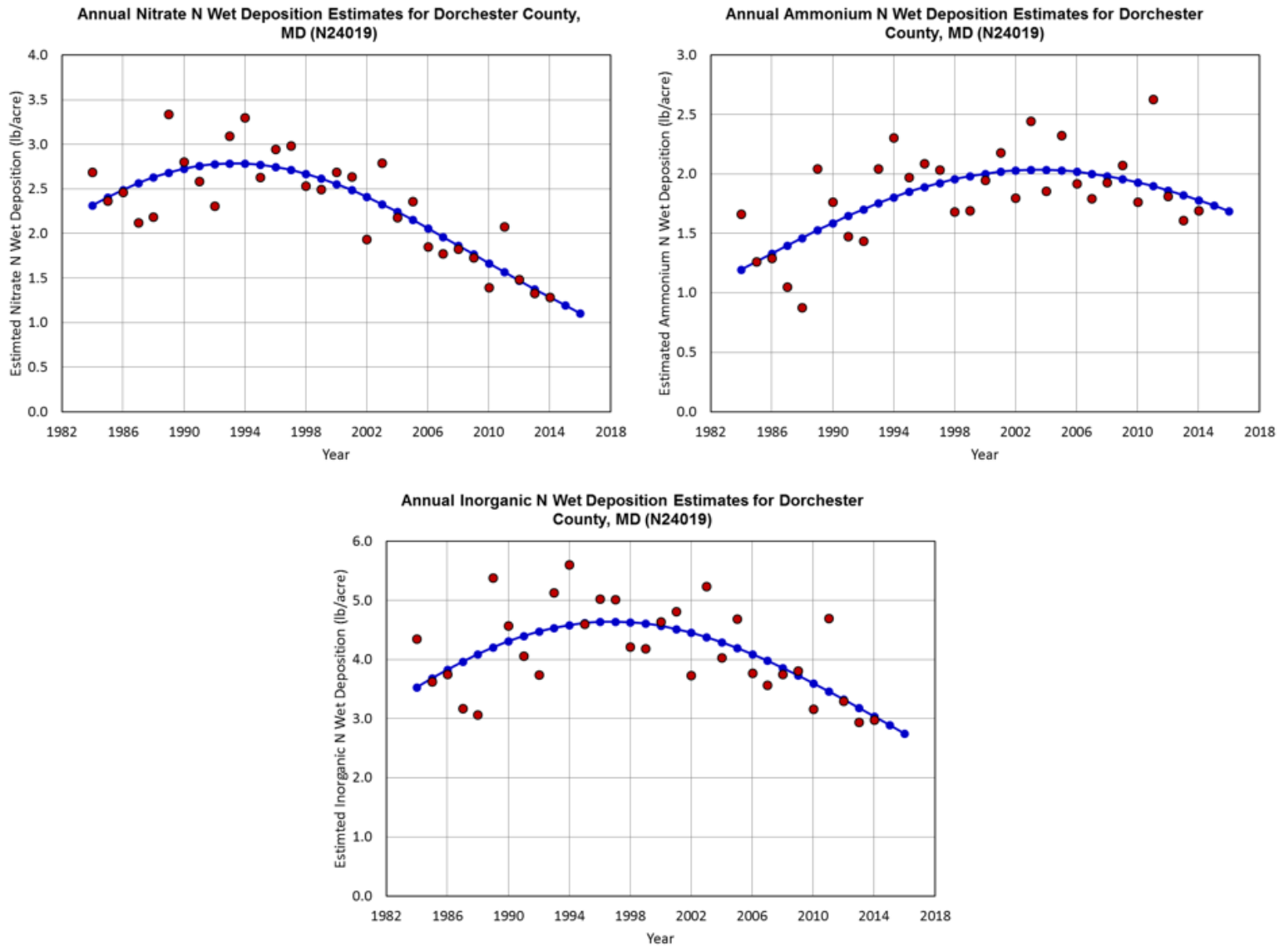

Figure 32. Long-term trends in annual nitrogen wet deposition estimates from the Phase 6 nitrate and ammonium models for Dorchester County, Maryland (Phase 6 land segment N24019).

Conclusions

The revised ammonium and nitrate wet-fall concentration models presented in this report were constructed from a set of NADP/NTN observations that was not only extended in historical scope, but also expanded in the number and range of environments sampled relative the models produced by our initial analyses (Grimm and Lynch, 2005; Grimm and Lynch, 2007). In spite of the increased diversity of the sample data set, the incorporation of additional detailed measures of land use, refined identification of emissions sources, an expanded set of meteorological parameters, and high-resolution tracking of emissions transport into the revised models maintained adequate model fit to the expanded precipitation event records and a net reduction in model estimation bias. Although the resulting wet-fall concentration functions are simpler in structure than those from our preceding study (Grimm and Lynch, 2007); they are expected to be more robust due to the much larger and diverse event sample set. The functional roles of the reduced set of model predictors in the revised models are more easily understood that in our previous models and can be directly related to physical phenomena and anthropogenic activities that are known to influence levels of ammonium and nitrate in precipitation.

One outcome that hasn't changed since our initial efforts to model ammonium and nitrate wet-fall concentrations across the CBW region is that precipitation volume is still, by far, the strongest factor determining single-event wet-fall concentrations of these inorganic nitrogen species. Because of the dominant role of precipitation volume in determining wet-fall concentrations of ammonium and nitrate and its inherent relationship to their rates of wet deposition, accurate precipitation data is critical to estimating the rates at which precipitation carries these ions to the surface.

This study involved an effort to assimilate information regarding the atmospheric transport of ammonia and nitrous oxides into models of ammonium and nitrate wet-fall concentration across the CBW region. The simple transport model employed in this study contributed significantly to the performance of the wet-fall concentration models and provided insight into how concentrations of the major inorganic nitrogen compounds found in precipitation are related to emissions from defined sets of point and area sources.

Literature Cited

Addiscott, T., 1983. Kinetics and temperature relationships of mineralization and nitrification in Rothamsted soils with differing histories. *Journal of Soil Science* **34**:343-353.

Ebisuzaki, W.. 2004. National Climatic Data Center Data Documentation for NOAA Operational Model Archive and Distribution System (NOMADS): North America Regional Reanalysis (NARR), Dataset DSI-6175. National Climatic Data Center, Asheville, NC. 11p.

Grimm, J.W. and J.A. Lynch. 2005. Improved daily precipitation nitrate and ammonium concentration models for the Chesapeake Bay watershed. *Environmental Pollution*, **135**(3):445-455.

Grimm, J.W. and J.A. Lynch. 2007. Refinements to the Daily Ammonium and Nitrate Wet-Fall Concentration Models for the Chesapeake Bay Watershed. Final Report to United States Environmental Protection Agency, Chesapeake Bay Program. Contract No. EPO63000212.

Harper, L.A. and R.R. Sharpe. 1997. Ammonia emissions and other nutrient transport in a swine production system. In: Proceedings of the Workshop on Atmospheric Nitrogen Compounds: Emissions, Transport, Transformation, Deposition and Assessment. North Carolina State University, Raleigh, NC, USA, pp. 242-258.

Valigura, R., Luke, W., Artz, R., Hicks, B., 1996. Atmospheric nutrient input to coastal areas – reducing the uncertainties. NOAA coastal ocean program decision analysis series, No. 9 (Silver Spring, MD).

Walker, J.T., V.P. Aneja, and D.A. Dickey. 1999. Atmospheric transport and wet deposition of ammonium in North Carolina. *Atmospheric Environment,* **34**(2000):3407-3418.

Xia, Y., et al. 2012, Continental-scale water and energy flux analysis and validation for the North American Land Data Assimilation System project phase 2 (NLDAS-2): 1. Intercomparison and application of model products, *J. Geophys. Res.*, 117, D03109.